Regulation of gliotoxin biosynthesis and protection in *Aspergillus* species

Patrícia Alves de Castro[1], Maísa Moraes[1], Ana Cristina Colabardini[1], Maria Augusta Crivelente Horta[1], Sonja L. Knowles[2], Huzefa A. Raja[2], Nicholas H. Oberlies[2], Yasuji Koyama[3], Masahiro Ogawa[3], Katsuya Gomi[4], Jacob L. Steenwyk[5], Antonis Rokas[5], Laure N.A. Ries[6*], and Gustavo H. Goldman[1*]

[1]Faculdade de Ciências Farmacêuticas de Ribeirão Preto, Universidade de São Paulo, Ribeirão Preto, Brazil

[2]Department of Chemistry and Biochemistry, University of North Carolina at Greensboro, North Carolina 27402, USA

[3]Noda Institute for Scientific Research, 338 Noda, Chiba 278-0037, Japan

[4]Department of Bioindustrial Informatics and Genomics, Graduate School of Agricultural Science, Tohoku University, Sendai, Japan.

[5]Department of Biological Sciences, Vanderbilt University, Nashville, Tennessee, USA

[6]MRC Centre for Medical Mycology at the University of Exeter, Geoffrey Pope Building, Exeter, UK

* Corresponding authors: rieslaure13@gmail.com and ggoldman@usp.br

Key words: *Aspergillus fumigatus*, *A. nidulans*, *A. oryzae*, gliotoxin, gliotoxin protection, transcription factors, mycotoxin

Abstract

Aspergillus fumigatus causes a range of human and animal diseases collectively known as aspergillosis. *A. fumigatus* possesses and expresses a range of genetic determinants of virulence, which facilitate colonisation and disease progression, including the secretion of mycotoxins. Gliotoxin (GT) is the best studied *A. fumigatus* mycotoxin with a wide range of known toxic effects that impair human immune cell function. GT is also highly toxic to *A. fumigatus* and this fungus has evolved self-protection mechanisms that include (i) the GT efflux pump GliA, (ii) the GT neutralising enzyme GliT, and (iii) the negative regulation of GT biosynthesis by the *bis*-thiomethyltransferase GtmA. The transcription factor (TF) RglT is the main regulator of GliT and this GT protection mechanism also occurs in the non-GT producing fungus *A. nidulans*. However, *A. nidulans* does not encode GtmA and GliA. This work aimed at analysing the transcriptional response to exogenous GT in *A. fumigatus* and *A. nidulans*, two distantly related *Aspergillus* species, and to identify additional components required for GT protection in *Aspergillus* species. RNA-sequencing shows a highly different transcriptional response to exogenous GT with the RglT-dependent regulon also significantly differing between *A. fumigatus* and *A. nidulans*. However, we were able to observe homologues whose expression pattern was similar in both species (43 RglT-independent and 12 RglT-dependent). Screening of an *A. fumigatus* deletion library of 484 transcription factors (TFs) for sensitivity to GT identified 15 TFs important for GT self-protection. Of these, the TF KojR, which is essential for kojic acid biosynthesis in *Aspergillus oryzae*, was also essential for GT biosynthesis in *A. fumigatus* and for GT protection in *A. fumigatus*, *A. nidulans*, and *A. oryzae*. KojR regulates *rglT* and *gliT* expression in *Aspergillus* spp. Together, this study identified conserved components required for GT protection in *Aspergillus* species.

Author Summary

A. fumigatus secretes mycotoxins that are essential for its virulence and pathogenicity. Gliotoxin (GT) is a sulfur-containing mycotoxin, which is known to impair several aspects of the human immune response. GT is also toxic to different fungal species, which have evolved several GT protection strategies. To further decipher these responses, we used transcriptional profiling aiming to compare the response to GT in the GT producer *A. fumigatus* and the GT non-producer *A. nidulans*. This analysis allowed us to identify additional genes with a potential role in GT protection. We also identified *A. fumigatus* 15 transcription factors (TFs) that are important for conferring resistance to exogenous gliotoxin. One of these TFs, KojR, which is essential for *A. oryzae* kojic acid production, is also important for GT protection in *A. fumigatus, A. nidulans* and *A. oryzae*. KojR regulates the expression of another TF and an oxidoreductase, previously shown to be essential for GT protection. Together, this work identified conserved components required for gliotoxin protection in *Aspergillus* species.

77 ## Introduction

78

79 *Aspergillus fumigatus* is a saprophytic fungus that can cause a variety of
80 human and animal diseases known as aspergillosis (Sugui *et al.*, 2014). The most
81 severe of these diseases is invasive pulmonary aspergillosis (IPA), a life-
82 threatening infection in immunosuppressed patients (van de Veerdonk *et al.*,
83 2017; Latgé and Chamilos, 2019). *A. fumigatus* pathogenicity is a multifactorial
84 trait that depends in part on several virulence factors, such as thermotolerance,
85 growth in the presence of hypoxic conditions, evasion and modulation of the
86 human immune system and metabolic flexibility (Kamei and Watanabe 2005;
87 Tekaia and Latgé 2005; Abad et al. 2010; Grahl et al. 2012; Latgé and Chamilos,
88 2019). Another important *A. fumigatus* virulence atribute is the production of
89 secondary metabolites (SMs). The genes that encode SMs are generally
90 organized in biosynthetic gene clusters (BGCs) (Keller, 2019) and *A. fumigatus*
91 has at least 598 SM-associated genes distributed among 33 BGCs (Lind *et al.*,
92 2017; Mead et al. 2019). SMs can cause damage to the host immune system,
93 protect the fungus from host immune cells, or can mediate the acquisition of
94 essential nutrients (Shwab et al. 2007; Losada et al. 2009; Yin et al. 2013;
95 Wiemann et al. 2014; Bignell et al. 2016; Knox et al. 2016; Raffa and Keller 2019;
96 Blachowicz et al. 2020). Gliotoxin (GT) is the best studied *A. fumigatus* SM and
97 has been detected *in vivo* in murine models of invasive aspergillosis (IA), in
98 human cancer patients (Lewis *et al.*, 2005), and is produced among isolates
99 derived from patients with COVID-19 (Steenwyk *et al.*, 2021).

100 Numerous modes of action for GT in the mammalian host have been
101 described: (i) GT interferes with macrophage-mediated phagocytosis through
102 prevention of integrin activation and actin dynamics, resulting in macrophage
103 membrane retraction and failure to phagocytose pathogen targets (Schlam *et al.*,
104 2016); (ii) GT inhibits the production of pro-inflammatory cytokines secreted by
105 macrophages and the activation of the NFkB regulatory complex (Arias *et al.*,
106 2018); (iii) GT interferes with the correct assembly of NADPH oxidase through
107 preventing p47phox phosphorylation and cytoskeletal incorporation as well as
108 membrane translocation of subunits p47phox, p67phox and p40phox (Tsunawaki

109 *et al.*, 2008); and (iv) GT inhibits neutrophil chemoattraction by targeting the
110 activity of leukotriene A4 (LTA4) hydrolase, an enzyme that participates in LTA
111 biosynthesis (König *et al.*, 2019).

112 GT is a sulfur-containing mycotoxin, a member of the
113 epipolythiopiperazines, produced by different fungal species, including
114 *Gliocadium fimbriatum* (from which it was originally isolated and named
115 accordingly), *A. fumigatus* and closely related non-pathogenic species (Knowles
116 *et al.*, 2020; Steenwyk *et al.*, 2020), and also by species of *Trichoderma* and
117 *Penicillium* (Scharf *et al.*, 2012, 2016; Welch *et al.* 2014; Dolan *et al.*, 2015). In
118 *A. fumigatus*, a BGC on chromosome VI contains 13 *gli* genes responsible for GT
119 biosynthesis and secretion (Dolan *et al.*, 2015). GT biosynthesis is tightly
120 regulated because it interferes with and depends on several cellular pathways
121 that regulate sulfur metabolism [cysteine (Cys) and methionine (Met)], oxidative
122 stress defenses [glutathione (GSH) and ergothioneine (EGT)], methylation [S-
123 adenosylmethionine (SAM)], and iron metabolism (Fe–S clusters) (Davis et
124 al.,2011; Struck et al., 2012; Amich et al., 2013; Sheridan et al.,
125 2016; Traynor et al., 2019). Regulation of GT biosynthesis involves numerous
126 transcription factors (TFs), protein kinases, transcriptional and developmental
127 regulators, regulators of G-protein signalling as well as chromatin modifying
128 enzymes (Dolan *et al*, 2015).

129 Even though the regulation of GT biosynthesis is well characterized,
130 regulation of endogenous protection from GT - which is also highly toxic to the
131 fungus - is less well understood. *A. fumigatus* self-protection against GT is
132 predicted to be based on the following mechanisms: (i) the major facilitator
133 superfamily transporter GliA, which is part of the GT BGC, catalyses GT efflux;
134 (ii) the reversible enzymatic activity of the oxidoreductase GliT, and (iii) the
135 negative regulation of GT biosynthesis through the off switch mechanism of the
136 *S*-adenosylmethionine-dependent gliotoxin *bis*-thiomethyltransferase GtmA. GliA
137 is responsible for transferring GT out of fungal cells and deletion of *gliA* increases
138 susceptibility to GT (Wang et al., 2014). GliT produces the final toxic form of GT
139 by catalysing disulphide bridge closure of the precursor dithiol gliotoxin (dtGT)
140 (Schrettl *et al.*, 2010; Dolan *et al.*, 2015). However, if there is excess GT
141 production, GliT is able to reduce GSH and produce dtGT attenuating GT toxicity

142 (Schrettl *et al.*, 2010; Dolan *et al.*, 2015). GtmA, whose gene is not located in the
143 GT BGC, is able to convert dtGT into bisdethiobis(methylthio)-gliotoxin (bmGT)
144 and to attenuate GT production postbiosynthetically (Dolan *et al.*, 2014, 2017;
145 Smith *et al.*, 2016; Scharf *et al.*, 2014). It is thought that the primary role of GtmA
146 is a decrease in GT biosynthesis and not a back up for GliT and toxin
147 neutralisation (Dolan *et al.*, 2015).

148 Until recently, the TF regulating *gliT* has remained elusive. The TF RglT
149 was shown to regulate not only GliZ, a Zn(II)2Cys6 transcription factor required
150 for gliotoxin biosynthesis, but several other *gli* genes, including *gliT*, which is not
151 regulated by GliZ (Schrettl *et al.*, 2010; Wang *et al.*, 2014; Dolan *et al.*, 2015; Ries
152 *et al.*, 2020), through directly binding to the respective promoter regions during
153 GT-producing conditions. Interestingly, RglT and GliT were shown to have similar
154 roles in GT protection in *A. nidulans*, a fungus that does not produce GT and is
155 distantly related to *A. fumigatus* (Ries *et al.*, 2020). The genome of *A. nidulans*
156 does not encode homologues for *gliA* and *gtmA*. Therefore, the aim of this work
157 is to compare the transcriptional response to exogenous GT in *A. fumigatus* and
158 *A. nidulans* and to further identify novel components required for GT protection in
159 *Aspergillus* species. By using transcriptional profiling (RNA-seq), we investigate
160 the influence of RglT in GT protection in the GT-producer *A. fumigatus* and in the
161 GT-non producer *A. nidulans*. We identified several novel genetic determinants
162 dependent or not on RglT and that could be involved in GT protection. We also
163 screened an *A. fumigatus* deletion library of 484 null mutants and identified, in
164 addition to RglT, 15 TFs that are potentially important for GT self-protection. We
165 found that one of these TFs is KojR, which is essential for *A. oryzae* kojic acid
166 production, is important for *A. nidulans* and *A. oryzae* GT protection and *A.*
167 *fumigatus* GT self-protection and GT and bmGT biosynthesis.

168

169 ## Results

170

171 ***A. fumigatus* RglT controls the expression of GT- and other SM-encoding**
172 **genes when exposed to exogenous GT.** To determine which genes are under

173 the transcriptional control of RglT in the presence of exogenous GT, we
174 performed RNA-sequencing (RNA-seq) of the *A. fumigatus* wild-type (WT) and
175 Δ*rglT* strains when exposed to 5 µg/ml GT for 3 h. In these conditions, *A.*
176 *fumigatus* is protecting itself from the effects of GT, as has previously been shown
177 (O'Keeffe *et al*., 2014). Differentially expressed genes (DEGs) were defined as
178 those with a minimum log2 fold change of 2 [log2FC ≥ 1.0 and ≤ -1.0; *p*-value <
179 0.05; FDR (false discovery rate) of 0.05]. DEG comparisons were carried out for:
180 (i) the WT strain, comparing the GT condition to the control (GT-free condition) to
181 determine which genes are modulated after 3 h exposure to GT; and (ii) when
182 comparing the *rglT* deletion strain to the WT strain in the presence of GT to
183 determine which genes are under the regulatory control of RglT in these
184 conditions.

185 In the WT strain, 260 genes were down-regulated and 270 genes up-
186 regulated when comparing the GT to the control condition (Supplementary Table
187 S1). FunCat (Functional Categorisation) (https://elbe.hki-
188 jena.de/fungifun/fungifun.php) analysis for the WT strain comparisons showed a
189 transcriptional up-regulation of genes coding for proteins involved in non-
190 vesicular ER transport, translation, mitochondrion, respiration and electron
191 transport (*p*-value < 0.01; Figure 1A). FunCat analysis for the down-regulated
192 genes showed enrichment for genes involved in homeostasis of metal ions,
193 detoxification involving cytochrome P450, C-compound and carbohydrate
194 metabolism, and secondary metabolism (*p*-value < 0.01; Figure 1A). When
195 comparing the WT to the Δ*rglT* strain in the presence of GT, a total of 269 genes
196 were down-regulated and 694 genes were up-regulated (Supplementary Table
197 S2). FunCat enrichment analysis of these DEGs showed a transcriptional up-
198 regulation of genes encoding proteins involved in secondary metabolism, C-
199 compound and carbohydrate metabolism, cellular import, and siderophore-iron
200 transport (*p*-value < 0.01; Figure 1B). FunCat analysis of down-regulated DEGs
201 showed enrichment of transport facilities, lipid, fatty acid and isoprenoid
202 metabolism, and homeostasis of cations (*p*-value < 0.01; Figure 1B). These
203 results suggest that *A. fumigatus* adapts to the prolonged presence of GT through
204 transcriptionally inducing cellular homeostasis and detoxification processes and
205 that RglT is important for these processes.

206 More specifically, RglT is important for the expression of 11 out of the 13
207 genes present in the GT BGC (including *gliT* and *gliA*) as well as *gtmA* (which is
208 not part of the GT BGC) in the presence of exogenous GT (Figure 1C).
209 Interestingly, *gliI* and *gliJ* expression is not altered by the presence of GT in the
210 WT and in the Δ*rglT* strains (Figure 1C), suggesting that the regulation of the
211 expression of these two genes is not affected by exposure to GT and are not
212 under the regulatory control of RglT. RNA-seq analysis also revealed
213 transcriptional modulation of other SM-encoding genes. For example, BGC
214 genes encoding components for the biosynthesis of pyripyropene,
215 naphthopyrone, fumagillin, fumiquinazolines, and fumigaclavine were shown to
216 be under the transcriptional control of RglT, with this TF repressing these genes
217 under prolonged GT exposing conditions (Figure 1D).

218 These results suggest that RglT is important not only for GT biosynthesis
219 and self-protection, but also for the regulation of the expression of genes involved
220 in the production of other SMs.

221

222 **Comparison of the *A. fumigatus* and *A. nidulans* transcriptional responses**
223 **when exposed to GT.** Next, we performed RNA-seq for the *A. nidulans* WT and
224 Δ*rglT* strains in the same conditions (5 µg/ml GT for 3 h) as described above.
225 DEGs were defined as those with a minimum log2 fold change of 2 [log2FC ≥ 1.0
226 and ≤ -1.0; *p*-value < 0.05; FDR (false discovery rate) of 0.05]. The same two
227 comparisons were carried out as described above for *A. fumigatus* (WT GT vs.
228 WT Control and Δ*rglT* GT vs WT GT). In the *A. nidulans* WT strain, 678 genes
229 were down-regulated and 675 genes were up-regulated when comparing the GT
230 to the control condition (Supplementary Table S3). We were not able to observe
231 any Funcat enrichment for these DEGs and then we employed gene ontology
232 (GO; https://elbe.hki-jena.de/fungifun/fungifun.php) enrichment analyses for the
233 WT strain that showed transcriptional up-regulation of genes coding for proteins
234 involved in mitochondrial function, such as ATP synthesis coupled proton
235 transport and cytochrome-c oxidase activity, as well as ergot alkaloid biosynthetic
236 process and a heterogeneous set of cellular components (*p*-value < 0.01; Figure
237 2A). GO analysis for the down-regulated genes showed enrichment for a

238 heterogeneous set of genes involved in biological processes and cellular
239 components (*p*-value < 0.01; Figure 2A). When comparing the WT to the Δ*rglT*
240 strain in the presence of GT, 132 genes were down-regulated and 68 genes were
241 up-regulated (Supplementary Table S4). GO enrichment analyses of the Δ*rglT*
242 strain showed a transcriptional up-regulation of genes encoding proteins involved
243 in nucleotide binding and cellular components (*p*-value < 0.01; Figure 2B). GO
244 analysis of down-regulated DEGs in the Δ*rglT* strain showed enrichment of flavin
245 adenine dinucleotide binding and oxidation-reduction processes (*p*-value < 0.01;
246 Figure 2B). In contrast to *A. fumigatus*, where prolonged exposure to GT resulted
247 in 530 identified DEG in the WT strain (about 5,3 % of the *A. fumigatus* 9,929
248 protein coding sequences, CDSs), in *A. nidulans* 1,353 DEG (about 13,5 % of the
249 *A. nidulans* 9,956 CDSs) were identified in the WT strain in these conditions.
250 Similarly, in *A. fumigatus*, RglT controls the expression of 963 genes (about 9,7
251 % of the CDSs) when exposed to GT for 3 h, whereas the number of genes
252 regulated by RglT in *A. nidulans* is smaller (200 genes, about 2 % of the CDSs).
253 Together, these results suggest very significant differences in the transcriptional
254 response to GT and for the role of RglT in mediating this response between
255 *Aspergilus* species.

256 To determine whether a conserved transcriptional response to GT in both
257 *A. fumigatus* and *A. nidulans* exists, we searched for homologous genes whose
258 expression pattern was similar (i) between the WT strains and (ii) RglT-dependent
259 in both fungal species in the presence of GT. When *A. fumigatus* wild-type DEGs
260 were compared to *A. nidulans* wild-type DEGs, 35 and 11 homologues were up-
261 and down-regulated in both species, respectively (Supplementary Table S3).
262 Furthermore, a total of 12 genes were found: six genes were dependent on RglT
263 for expression [GliT (AN3963/AFUA_6G09740), a methyltransferase
264 (AN3717/AFUA_6G1278), GprM (AN3567/AFUA_7G05300), a Major Facilitator
265 Superfamily transporter (AN1472/AFUA_8G04630), AN8167/AFUA_5G02950,
266 and AN1470/AFUA_5G8G04260 with unknown functions]; and the other six
267 genes were dependent on RglT for repression [lysozyme activity
268 (AN6470/AFUA_6G10130), L-PSP endoribonuclease
269 (AN5543/AFUA_5G033780), oxidoreductase activity (AN3279/AFUA_5G09290
270 and AN9051/AFUA_7G00700), NmrA-transcription factor

271 (AN9531/AFUA_7G06920), and an ATP-binding cassette transporter
272 (AN7879/AFUA_1G10390)] (Figure 2C and Supplementary Table S4).

273 We observed 43 homologues that were RglT-independent (Supplementary
274 Table S4) and among them, we identified as induced by GT a putative cysteine
275 synthase (AN7113/AFUA_4G03930) and ZrcA, a zinc/cadmium resistance
276 protein (AN10876/AFUA_7G06570) (Supplementary Table S4). Another RglT-
277 independent gene is the GliT homologue AN6963/AFUA_5G03540; interestingly,
278 this gene is upregulated in *A. nidulans* and downregulated in *A. fumigatus* upon
279 GT exposure (Supplementary Table S4).

280 RNA-seq results were confirmed by RT-qPCR for the majority of the 9
281 selected *A. fumigatus/A. nidulans* homologues and for the *A. fumigatus* GtmA-
282 encoding gene (*A. nidulans* lacks a homologue) (Figures 2D and 2E and
283 Supplementary Figure S1). The expression of these 10 genes showed a high
284 level of correlation with the RNA-seq data (Pearson correlation from 0.896 to
285 0.952; Figure 2E).

286 Taken together, our results suggest that the transcriptional response of *A.*
287 *fumigatus* and *A. nidulans* to GT is very different, although we were able to
288 observe 55 homologues shared between both species.

289

290 **Screening of *A. fumigatus* TF deletion strains for sensitivity to GT.** Our RNA-
291 seq results suggest there are DEGs that are not dependent on RglT and could
292 be important for GT protection in *Aspergilli*. To identify TFs involved in the GT
293 self-protection response, we took advantage of the existing *A. fumigatus* TF null
294 deletion library (Furukawa *et al.*, 2020) which we screened for sensitivity to 35
295 µg/ml of GT (*A. fumigatus* minimal inhibitory concentration for GT is 70 µg/ml). In
296 addition to Δ*rglT*, 15 null mutants exhibited increased sensitivity to 35 µg/ml of
297 GT [ΔAFUA_06800 (Δ*kojR*), ΔAFUA_2G17860, ΔAFUA_3G13920 (Δ*rgdA*),
298 ΔAFUA_5G12060, ΔAFUA_5G11260 (Δ*sreA*), ΔAFUA_8G07360,
299 ΔAFUA_8G07280, ΔAFUA_4G13060, ΔAFUA_5G14390, ΔAFUA_6G09870,
300 ΔAFUA_3G01100, ΔAFUA_8G03970, ΔAFUA_6G09930 (Δ*yap1*),
301 ΔAFUA_3G09670 (Δ*oefC*), and ΔAFUA_8G05460] (Table 1 and Figure 3). Only
302 AFUA_3G09670 (*oefA*) is up-regulated in the Δ*rglT* mutant and only

303 AFUA_4G13060 is up-regulated in the wild-type strain in our RNA-seq
304 experiments (Supplementary Tables S1 and S2).

305 Previous studies have shown that GT biosynthesis and self-protection is
306 intimately linked to sulfur metabolism, oxidative stress resistance, as well as iron
307 and zinc metabolism (Mukherjee *et al.* 2018; Winkelströter *et al.*, 2015; Jain *et*
308 *al.*, 2011; Seo *et al.*, 2019; Vicentefranqueira *et al.*, 2018; Traynor *et al.*, 2018).
309 To identify if any of the TFs identified in the screen are associated with these
310 pathways, the null mutants were screened for growth in the presence of (i)
311 methionine or cysteine as single sulfur sources; (ii) oxidative stress-inducing
312 agents such as allyl alcohol (converted to the oxidative stress-inducing
313 compound acrolein by alcohol dehydrogenases), *t*-butyl hydroxyperoxide,
314 menadione, and diamide (a GSH scavenger); and (iii) increased and depleted
315 extracellular iron and zinc concentrations (Figure 4). None of these mutants
316 showed altered growth compared to the WT strain in the presence of methionine
317 or cysteine as single sulfur sources (Supplementary Figure S2). Six of the
318 deletion strains [Δ*rglT*, Δ*sreA* (ΔAFUA_5G12060), ΔAFUA_5G140390, Δ*yap1*
319 (ΔAFUA_6G09930), ΔAFUA_6G09870, and ΔAFUA_8G07360] were sensitive to
320 at least one of the four oxidative stress-inducing agents (Figures 4A to 4D).
321 Interestingly, ΔAFUA_8G07360 is resistant to diamide (Figure 4D). Four strains
322 (ΔAFUA_3G13920, ΔAFUA_5G11260, ΔAFUA_3G01100 and
323 ΔAFUA_8G03970) had increased growth, while ΔAFUA_3G09670,
324 ΔAFUA_5G06800, and ΔAFUA_5G12060 presented significantly decreased
325 growth in iron starvation conditions (Figures 4F). Intriguingly, ΔAFUA_8G05460
326 had reduced growth upon zinc starvation but increased growth upon zinc excess
327 (Figures 4G and 4H). The Δ*rglT* mutant has reduced growth in zinc starvation
328 conditions but had increased growth in iron starvation conditions (Figures 4F and
329 4H).

330 Taken together, these results strongly suggest that some of the mutants
331 identified as more sensitive to GT are also involved in pathways related to
332 oxidative stress and iron and zinc metabolism.

333

334 **Production of gliotoxin and BmGT in the gliotoxin sensitive mutants.** The
335 Δ*rglT* and Δ*gliT* strains are not only sensitive to exogenous GT, but they also
336 secrete significantly less GT (Schrettl *et al.*, 2010; Ries *et al.*, 2020). To determine
337 if the TF deletion strains from our screen are also impaired for GT and bmGT
338 biosynthesis and secretion, we quantified extracellular GT and bmGT in culture
339 supernatants of these strains when grown in GT-inducing conditions. As
340 previously demonstrated (Ries *et al.*, 2020), high performance liquid
341 chromatography and mass spectrometry experiments showed that Δ*rglT* has
342 reduced GT and produces a similar of bmGT when compared to the WT and *rglT*
343 complemented strains (Supplementary Table S5, Figures 5A to 5C). The Δ*kojR*
344 (ΔAFUA_5G06800), ΔAFUA_2G17860, Δ*rgdA* (ΔAFUA_3G13920),
345 ΔAFUA_5G12060, Δ*sreA* (ΔAFUA_5G11260), and ΔAFUA_8G07360 strains
346 secrete significantly less GT when compared to the WT strain (Figures 5A and
347 5C). In contrast, the ΔAFUA_8G03970, ΔAFUA_6G09930, and Δ*oefC*
348 (ΔAFUA_3G09670) strains secrete significantly more GT than the WT strain
349 (Figures 5A and 5C). Production of bmGT is decreased in the Δ*kojR*
350 (ΔAFUA_5G06800) but increased in most of the strains (10 out of 16), with the
351 exception of Δ*rglT*, ΔAFUA_2G17860, ΔAFUA_3G13920, ΔAFUA_5G12060, and
352 Δ*sreA* (ΔAFUA_5G11260) which produce similar concentrations of bmGT than
353 the WT strain (Figures 5B and 5C). Interestingly, the Δ*kojR* (ΔAFUA_5G06800)
354 strain is the only TF deletion strain with reduced GT and bmGT levels (Figures
355 5A to 5C), whilst the ΔAFUA_8G03970, ΔAFUA_6G09930, and Δ*oefC*
356 (ΔAFUA_3G09670) strains have increased levels of GT and bmGT in the
357 supernatants (Figures 5A to 5C).

358 Our results indicate that several TFs are involved in the induction or
359 repression of GT and bmGT biosynthesis. In contrast, only for the Δ*kojR* strain
360 are GT and bmGT extracellular levels significantly decreased, and we have
361 chosen this TF for further characterisation.

362

363 **RglT and KojR are important for GT protection in *Aspergilli*.** We have
364 previously shown that RglT and GliT in *A. fumigatus* and *A. nidulans* have a
365 similar role in protecting each fungus from the deleterious effects of GT (Ries *et*
366 *al.*, 2020). Homologues of RglT and GliT are present in a number of

367 Eurotiomycetes and Sordariomycetes suggesting that this mechanism of GT
368 protection is widespread, including in many species that are not GT producers
369 (Ries *et al*., 2020). Phylogenetically informed model testing led to an evolutionary
370 scenario in which the GliT-based resistance mechanism is ancestral and RglT-
371 mediated regulation of GliT occurred subsequently (Ries *et al*., 2020). To
372 determine whether a phylogenetic relationship exists between RglT and KojR, we
373 screened for the presence of GT and kojic acid BGCs as well as RglT and KojR
374 homologues across *Aspergillus* and *Penicillium* species and constructed a
375 phylogenetic tree (Figure 6A). Results suggest that their origins predate the origin
376 of both genera. In contrast, homologues of the kojic acid BGC are present in only
377 *A. oryzae* and close relatives (Figure 6A). In contrast to RglT and GliT,
378 examination of the phylogenetic distribution patterns of RglT and KojR revealed
379 that they are not significantly correlated (scenario A). The same was true for KojR
380 and the kojic acid BGC, suggesting that KojR was recruited specifically for kojic
381 acid biosynthesis in *A. oryzae* and close relatives. In contrast, the distribution of
382 the GT biosynthetic gene cluster is correlated with the presence of *RglT* (scenario
383 B; Ries et al., 2020), but not vice-versa; however, scenario A (lack of correlation
384 between their distributions) also fit the observed data well (Table 2).

385 To determine whether KojR is also required for protection from GT in other
386 fungi, the corresponding homologous genes were deleted in *A. nidulans* (chosen
387 because it does not produce either GT or kojic acid) and *A. oryzae* (produces
388 kojic acid). Similarly to *A. fumigatus*, deletion of *kojR* significantly increased
389 sensitivity to exogenously added GT in all three species (Figures 6B, 6C and 6D).
390 In contrast to the deletion of *rglT*, deletion of *kojR* still conferred some resistance
391 to exogenous GT (Figures 6B, 6C and 6D), suggesting that RglT functions
392 downstream of KojR and/or that RglT is regulated by KojR in these conditions.
393 To address this, the *A. oryzae* WT, the *rglT* and the *kojR* deletion strains were
394 first screened for kojic acid production, which can be seen by the intensity of the
395 red color (formed by chelating ferric ions) on plates. As expected, deletion of *kojR*
396 resulted in the absence of red colour and hence kojic acid production, whereas
397 deletion of *rglT* did not affect kojic acid production in *A. oryzae* (Figure 6E). These
398 results suggest that RglT does not regulate kojic acid production in *A. oryzae*. To
399 determine whether *rglT* is under the transcriptional control of KojR in the presence

400 of GT, *rglT* transcript levels were quantified by RT-qPCR in the WT and *kojR*
401 deletion strains (Figure 7A). In the *A. fumigatus* and *A. oryzae* Δ*kojR* strains, *rglT*
402 transcript levels were significantly reduced, suggesting that KojR regulates *rglT*
403 expression in the presence of exogenous GT (Figure 7A). To determine whether
404 KojR is under the transcriptional control of RglT in the presence of GT,
405 transcriptional levels of *kojR* in the *A. fumigatus* and *A. oryzae rglT* deletion
406 strains were measured by RT-qPCR (Figure 7B). In *A. fumigatus* and *A. oryzae*,
407 deletion of *rglT* resulted in significantly decreased and increased *kojR* transcript
408 levels, respectively, suggesting that RglT regulates *kojR* in these fungi. We were
409 unable to measure the expression levels of *A. nidulans kojR* and *rglT* in the
410 absence or presence of GT because the PCR amplification profiles were similar
411 to the negative control (water), suggesting *kojR* and *rglT* have very low levels of
412 expression in this fungus.

413 Finally, we further assessed the role of KojR in GT protection in *A.*
414 *fumigatus*, *A. nidulans*, and *A. oryzae*. We were unable to detect any GT and
415 bmGT production in *A. oryzae* wild-type, RglT and KojR (Supplementary Figure
416 S3). We previously demonstrated that the expression of *gliT*, encoding an
417 oxidoreductase with a GT neutralising function, is dependent on RglT in both *A.*
418 *fumigatus* and *A. nidulans* when GT was added exogenously to the medium (Ries
419 *et al*., 2020; Figures 2C and 7C). In agreement with these data, the expression
420 of *A. oryzae gliT* is decreased in the Δ*rglT* mutant, suggesting that *gliT* expression
421 is dependent on RglT in all three *Aspergillus* species (Figure 7C). Furthermore,
422 *gliT* expression was also dependent on KojR in these fungal species with KojR
423 inducing *gliT* expression in *A. fumigatus* and *A. oryzae* and repressing *gliT* in *A.*
424 *nidulans* (Figure 7E). Subsequently, *gtmA* transcript levels were also quantified
425 as *gtmA* is also important for GT self-protection (Dolan *et al*., 2014). The
426 expression of *gtmA* is also decreased in both the *A. fumigatus* and *A. oryzae*
427 Δ*rglT* and Δ*kojR* mutants (Figures 7D and 7F). No *gtmA* homologue is present in
428 *A. nidulans*.

429 Together these results suggest: (i) a regulatory interplay exists between
430 RglT and KojR in GT protection that differs between *Aspergillus* spp; (ii) RglT-
431 dependent GliT protection from exogenous GT is a conserved mechanism in GT-
432 producing and non-producing *Aspergillus* spp; (iii) GT protection mechanisms

433 appear to be similar in GT-producing *Aspergillus* spp; and (iv) the existence of
434 further mechanisms of GT self-protection that significantly differ between GT-
435 producing and non-producing *Aspergillus spp*.

436

437 ## Discussion

438

439 The transcriptional regulation of GT biosynthesis requires many
440 components including TFs, protein kinases, G-protein signalling and chromatin
441 modifying enzymes, which together integrate different signaling pathways (Dolan
442 et al., 2015). In addition, GT biosynthesis requires GSH, of which the sulfur-
443 containing amino acids methionine and cysteine are biosynthetic precursors; and
444 GT biosynthesis is linked to cellular oxidative stress in mammalian and fungal
445 cells via a yet to be described mechanism (Davis et al., 2011; Struck et al., 2012;
446 Amich et al., 2013; Sheridan et al., 2016; Traynor et al., 2019). In addition, GT
447 self-protection is essential during GT biosynthesis. The three main mechanisms
448 of GT self-protection in *A. fumigatus* are the GT-neutralising oxidoreductase GliT,
449 the GT efflux pump GliA, and the negative regulation of GT biosynthesis through
450 GtmA (Dolan *et al.*, 2015). RglT was recently identified as the main TF controlling
451 the expression of *gliT* and of *gtmA* in *A. fumigatus*. The RglT homologue is also
452 important for *gliT* expression and GT protection in the non-GT producer *A.*
453 *nidulans* (Ries *et al.*, 2020). Despite this similarity, *A. nidulans* does not encode
454 homologues of GtmA and GliA, suggesting that (i) these GT protection
455 mechanisms are not required or that (ii) additional, unknown GT protection
456 mechanisms exist in this fungus. It is perhaps not surprising that GtmA and GliA
457 are not present in *A. nidulans*, because as a non-GT producing fungus, GtmA-
458 mediated attenuation of GT biosynthesis and GT efflux are not required. We
459 currently do not know how the presence of GT is signalled and/or whether this
460 mycotoxin can be taken up by *A. nidulans*. In this work, the transcriptional
461 response of *A. fumigatus* and *A. nidulans* upon prolonged exposure to GT was
462 analysed and found to be significantly different between both fungal species. In
463 agreement, the RglT-dependent regulome in both fungal species is also very
464 different. This may be due to the evolutionary distance between both fungal

465 species which share around 66-67% of amino acid identity, a protein identity
466 comparable to the phylogenetic relationship between mammals and fish
467 (Galagan et al., 2005). Despite this, our dataset also identified a conserved
468 transcriptional response. These genes encode proteins important for gliotoxin
469 modification, such as the observed RglT-dependent putative methyltransferase
470 (AN3717/AFUA_6G1278) and two putative oxidoreductases
471 (AN3279/AFUA_5G09290 and AN9051/AFUA_7G00700), attenuating directly or
472 indirectly its activity. The importance of these genes in these processes remains
473 to be investigated.

474 To further identify conserved components important for GT self-protection,
475 we screened the *A. fumigatus* TF deletion library to identify TFs important for this
476 process. We identified 15 TFs (4 have been characterized and 11 have not been
477 characterized), whose deletion caused a significant decrease in growth in the
478 presence of exogenous GT. The 11 uncharacterized TFs can broadly be classed
479 into 4 categories based on their respective GT and bmGT biosynthesis profiles:
480 (i) AFUA_2G17860 and AFUA_5G12060 (whose deletion mutants are GT non-
481 producers and bmGT producers), (ii) AFUA_3G01100, AFUA_5G14390,
482 AFUA_4G13060, AFUA_6G09870, AFUA_8G07280 and AFUA_8G05460
483 (whose deletion mutants are GT producers and bmGT overproducers), (iii)
484 AFUA_8G03970 and *oefC* (AFUA_3G09670, whose deletion mutants are GT and
485 bmGT overproducers) and (iv) AFUA_8G07360 (whose deletion mutant is a GT
486 non-producer and bmGT overproducer). They present interesting targets for
487 future mycotoxin-related studies.

488 In addition, our work identified an additional 4 TFs, which have previously
489 been characterized, as important for GT biosynthesis. Yap1 (AFUA_6G09930,
490 whose deletion mutant is a GT overproducer and bmGT overproducer) is an
491 important regulator of resistance to oxidative stress (Qiao *et al.*, 2008). SreA
492 (AFUA_5G11260, whose deletion mutant is a GT non-producer and bmGT
493 producer) regulates iron uptake, through repressing iron-regulated genes and
494 siderophore biosynthesis genes in high-iron conditions (Schrettl *et al.*, 2008). The
495 identification of these TFs emphasizes the close connection between GT
496 production and oxidative stress and iron metabolism (Dolan *et al.*, 2015;
497 Winkelströter *et al.*, 2015; Jain *et al.*, 2011; Sheridan *et al.*, 2016). RgdA

498 (AFUA_3G13920, whose deletion mutant is a GT non-producer and bmGT
499 producer) has previously been reported as important for hyphal growth, asexual
500 sporulation and virulence (Jun *et al.*, 2020). In contrast to our results, these
501 authors observed increased GT production in the Δ*rgdA* mutant, which may be
502 due to the fact they have used Af293 as a background strain for the *rgdA* deletion
503 mutant whereas this work used CEA17 as a background strain (Jun *et al.*, 2020).
504 Differences in cellular responses between these two *A. fumigatus* background
505 strains have been reported before and include the role of the calcium-responsive
506 TF CrzA during the caspofungin paradoxical effect (Ries et al., 2017). KojR
507 (AFUA_5G06800, whose deletion mutant is a GT non-producer and bmGT non-
508 producer) is the *A. oryzae* homologue involved in the production of kojic acid
509 (Terabayashi *et al*, 2010). It is perhaps not surprising that our work identified
510 Yap1, SreA and RgdA as involved in GT biosynthesis and self-protection, as
511 oxidative stress, iron metabolism, and fungal growth have all been shown to be
512 important for GT and/or SM biosynthesis (Dolan *et al.*, 2015; Winkelströter *et al.*,
513 2015; Jain *et al.*, 2011; Sheridan *et al.*, 2016). In contrast, the deletion of *kojR*
514 was the only mutant strain where no GT and bmGT was observed, suggesting
515 that this TF is important for GT metabolism. The role of this TF in GT protection
516 was therefore further characterised in GT-producing *A. fumigatus* and non-
517 producing (*A. nidulans* and *A. oryzae*) *Aspergillus* species. These results expand
518 significantly the number of TFs involved, and suggest additional complex
519 mechanisms in regulating GT protection and production. These results expand
520 significantly the number of TFs involved in GT biosynthesis and self-protection,
521 and suggest additional complex mechanisms in regulating the processes.

522 We were able to show a conserved mechanism of protection from GT in
523 these three fungi whereby deletion of *kojR* and *rglT* increases sensitivity to
524 exogenous GT. This protection is likely to occur through the RglT-dependent
525 regulation of GliT, where expression of *gliT* is dependent on RglT in the presence
526 of GT in the three fungal species. Future studies will determine growth of the
527 respective *gliT* deletion strains in order to confirm this conserved mechanism of
528 GT protection in *Aspergillus* species. The expression of *gliT* is also dependent on
529 KojR in all three fungi in the presence of GT; however, KojR is required for *gliT*
530 expression in the GT-producing fungi *A. fumigatus* and *A. nidulans*, whereas KojR

531 represses *gliT* in *A. nidulans*, which does not produce GT. These results suggest
532 that KojR-dependent regulation of *gliT* differs between GT-producing and non-
533 producing *Aspergillus* species and these results are in agreement with our *A.*
534 *fumigatus*/*A. nidulans* RNA-seq dataset. It remains to be determined how KojR
535 protects *A. nidulans* from GT if this does not involve the expression of GliT. It is
536 possible that another oxidoreductase is involved in GT self-protection. Indeed
537 several oxidoreductase-encoding genes were identified as highly up-regulated in
538 our RNA-seq dataset, although their function remains to be determined.

539 Adding to this complexity, is the interplay of regulation between the TFs
540 RglT and KojR in the presence of GT. Unfortunately we could not detect
541 significant levels of *rglT* and *kojR* in *A. nidulans* in these conditions and thus the
542 mechanism of how RglT, KojR, and GliT confer GT protection in this GT non-
543 producing fungus remains unknown. In *A. fumigatus* and *A. oryzae*, *rglT*
544 expression is dependent on KojR and we suggest here that KojR directly
545 regulates *rglT* and indirectly *gliT*. This regulatory hierarchy would therefore confer
546 protection from GT in these fungi. Future experiments will include binding targets
547 of KojR in order to confirm this hypothesis. In *A. fumigatus, kojR* expression is
548 dependent on RglT whereas in *A. oryzae kojR* repression is dependent on RglT.
549 These results suggest that differences in the regulation of both TFs in these fungi.

550 Although *A. oryzae* has the GT BGC, we were unable to detect GT
551 production in the *A. oryzae* wild-type, Δ*rglT* and Δ*kojR* strains (Supplementary
552 Figure S3). Since in *A. fumigatus*, *gliT* and *gtmA* expression are not dependent
553 on GliZ, a possible explanation for not detecting GT production is that GT
554 production and secretion was lost in *A. oryzae.* However, RglT and KojR are still
555 regulating *A. oryzae gliT* and *gtmA*. *A. oryzae* strains have been selected for
556 millenia for the saccharification of starch-rich rice to sugars that are fermentable
557 by *S. cerevisiae* into sake, the high-alcohol rice wine (Yoshizawa, 1999). The *A.*
558 *oryzae*-rice mixture (*koji*-culture) is mixed with additional steamed rice and
559 fermented by *S. cerevisiae*. This *A. oryzae* rice starch breakdown and
560 subsequent conversion into alcohol by *S. cerevisiae* occurs side by side
561 (Yoshizawa, 1999). Extensive genome analysis suggested that, through selection
562 by humans, atoxigenic lineages of *A. oryzae* evolved into “cell factories” important
563 for the saccharification process (Gibbons *et al.*, 2012). Interestingly, production

564 of the secondary metabolite kojic acid was retained in these strains during the
565 *koji*-culture (Terabayashi *et al*, 2010). The kojic acid gene cluster is one of the
566 simplest clusters of secondary metabolite production ever reported, composed
567 by three genes: an enzyme containing a FAD-dependent oxidoreductase domain,
568 a transporter, and a *kojR* encoding a GAL4-like Zn(II)2Cys6 transcription factor
569 (Terabayashi *et al*, 2010; Rokas *et al.*, 2018). As expected, *A. oryzae* Δ*kojR* is
570 unable to produce kojic acid (Terabayashi *et al*, 2010) but there is no involvement
571 of RglT in kojic acid production. Interestingly, we observed that both *A. fumigatus*
572 and *A. oryzae* Δ*rglT* and Δ*kojR* are more sensitive to GT and involved in the
573 positive regulation of the oxidoreductase *gliT* and *gtmA*. Although *gliT* expression
574 is reduced in *A. nidulans* Δ*rglT*, it is increased in Δ*kojR*, suggesting the
575 mechanism of *gliT* regulation is distinct in this species. Since GliT is essential for
576 *A. nidulans* GT detoxification, these results indicate that increased expression of
577 *gliT* in the *A. nidulans* Δ*kojR* strain is not enough to confer GT resistance to *A.*
578 *nidulans*. These results suggest that KojR is also important for GT detoxification
579 in a GT non-producer and that there are additional mechanisms of GT
580 detoxification regulated by KojR in *A. nidulans*.

581 Our work provides new opportunities to understand GT production and
582 protection, and also highlights significant differences in transcriptional responses
583 to extracellular mycotoxins between fungal species. More importantly, the
584 identification of a conserved transcriptional response to exogenous GT in
585 different *Aspergillus* species provides a basis for future studies which will further
586 decipher these protection pathways, potentially leading to the development of
587 anti-fungal strategies.

588

589 ## Materials and Methods

590

591 **Strains and media.** All strains used in this study are listed in Supplementary
592 Table S6. Strains were grown at 37 °C except for growth on allyl alcohol-
593 containing solid medium, which was carried out at 30°C. Conidia of *A. fumigatus*
594 and *A. nidulans* were grown on complete medium (YG) [2% (w/v) glucose, 0.5%
595 (w/v) yeast extract, trace elements] or minimal media (MM) [1% (w/v) glucose,

596 nitrate salts, trace elements, pH 6.5]. Solid YG and MM were the same as
597 described above with the addition of 2% (w/v) agar. Where necessary, uridine
598 and uracil (1.2 g/L) were added. Trace elements, vitamins, and nitrate salt
599 compositions were as described previously (KAFER, 1977). Potato Dextrose
600 Agar (PDA, Difco™) was used for *A. oryzae*. For iron or zinc starvation or excess
601 experiments, strains were growth in solid MM without $FeSO_4$ or zinc. For
602 phenotypic characterization, plates were inoculated with 10^4 spores per strain
603 and left to grow for 120 h at 37 or 30 °C. All radial growth experiments were
604 expressed as ratios, dividing colony radial diameter of growth in the stress
605 condition by colony radial diameter in the control (no stress) condition.
606
607 **Phylogenomic inference of *Aspergillus* – *Penicillium* species phylogeny.**
608 Publicly available gene annotations for *Aspergillus* and *Penicillium* species
609 (n=55) were downloaded from NCBI in February 2021. OrthoFinder, v2.3.8
610 (Emms and Kelly, 2019), was used to identify orthologous groups of genes using
611 the protein sequences of the 55 proteomes as input. From the 18,979 orthologous
612 groups of genes, 1,133 were identified to be single-copy and present in all
613 proteomes. All 1,133 genes were aligned using MAFFT, v7.402 (Katoh and
614 Standley, 2013), with the 'auto' option. The corresponding nucleotide sequences
615 were threaded onto the protein alignments using the 'thread_dna' function in
616 PhyKIT, v1.1.2 (Steenwyk et al., 2021). The resulting nucleotide alignments were
617 trimmed using ClipKIT, v1.1.3 (Steenwyk et al., 2020), with the 'smart-gap' option.
618 All 1,133 genes were concatenated into a single matrix with 2,446,740 sites using
619 the 'create_concat' function in PhyKIT (Steenwyk et al., 2021). The resulting
620 alignment was used to reconstruct the evolutionary history of the 55 species using
621 IQ-TREE, v2.0.6 (Minh et al., 2020). During tree search, the number of trees
622 maintained during maximum likelihood inference was increased from five to ten
623 using the 'nbest' option. Bipartition support was assessed using 1,000 ultrafast
624 bootstrap approximations (Hoang et al., 2018).

625 Comparison of the inferred phylogeny showed that it was nearly identical to the
626 phylogeny inferred in a previous genome-scale examination of evolutionary
627 relationships among *Aspergillus* and *Penicillium* species (Steenwyk et al., 2019).
628 Minor differences were observed among bipartitions previously determined to

629 harbor high levels of incongruence. These differences concern the placements of
630 *Penicillium decumbens* and *Aspergillus awamori*. Differences in gene and taxon
631 sampling may be responsible for these incongruences. All bipartitions received
632 full support.

633

634 **Identifying homologous biosynthetic gene clusters and orthologs of *RglT***
635 **and *kojR.*** To identify homologs of the biosynthetic gene clusters involved in the
636 production of gliotoxin and kojic acid, the 13 protein sequences of the gliotoxin
637 cluster from *Aspergillus fumigatus* and the three protein sequences of the kojic
638 acid cluster from *Aspergillus oryzae* were used as queries during sequence
639 similarity searches to identify homologs in the 55 proteomes. Sequence similarity
640 searches were conducted using NCBI's blastp function from BLAST+, v 2.3.0
641 (Camacho et al., 2009), with an expectation value threshold of 1e-4. Across all
642 homologs, the physical proximity of each gene was assessed. We considered
643 biosynthetic gene clusters to be homologous if 7 / 13 genes from the gliotoxin
644 biosynthetic gene cluster were present including the nonribosomal peptide
645 synthase, *gliP*. For the kojic acid biosynthetic gene cluster, we required that 2 / 3
646 genes from the kojic acid cluster were present including *kojA*, the oxidoreductase
647 required for kojic acid production (Tamano *et al.*, 2019). When examining gene
648 proximity, a gene boundary distance of five genes was used. To identify genes
649 orthologous to *RglT* and *kojR*, OrthoFinder results were parsed to identify genes
650 in the same orthologous group as each gene.

651

652 **Testing the association of the phylogenetic distributions of *kojR* and *RglT.***
653 To evaluate if the distributions of *kojR*, *RglT*, and their BGCs on the species
654 phylogeny are significantly associated, we examined the correlation of the
655 phylogenetic distribution of the presence and absence patterns of the two genes
656 on the species phylogeny. We used Pagel's binary character correlation test
657 implemented in phytools, v0.7-70 (Revell, 2012) to examine four scenarios: the
658 distributions of two genes / BGCs are not correlated (scenario A), the distribution
659 of one gene is correlated with the distribution of another gene / BGC but not vice
660 versa (scenarios B and C), and the distributions of two genes / BGCs are

661 correlated (scenario D). The best fitting model was then determined using the
662 weighted Akaike information criterion (AIC).

663

664 **Generation of deletion mutants for *A. oryzae kojR* and *rglT, A. nidulans kojR***
665 **and *A. fumigatus ΔkojR::kojR*$^{+}$**.. The DNA fragment for *kojR* deletion, using the
666 *A. oryzae* orotidine-5′-decarboxylase gene (*pyrG*) as a selectable marker, was
667 generated by fusion polymerase chain reaction (PCR) as follows: DNA fragments
668 upstream and downstream of the *kojR* coding region were amplified by PCR
669 using *A. oryzae* genomic DNA as a template and the primer sets BR-TF040-L-F
670 + BR-TF040-L-R and BR-TF040-R-F + BR-TF040-R-R, respectively. The *pyrG*
671 fragment was amplified by PCR using *A. oryzae* genomic DNA as a template and
672 the primers BR-TF040-P-F and BR-TF040-P-R. Then, these three PCR
673 fragments were mixed, and a second round of PCR with the primers BR-TF040-
674 L-F and BR-TF040-R-R was performed. For *rglT* deletion, DNA fragments
675 upstream and downstream of the *rglT* coding region were amplified by PCR using
676 the primer sets BR-TF390-L-F + BR-TF390-L-R and BR-TF390-R-F + BR-TF390-
677 R-R, respectively. The *pyrG* fragment was amplified by PCR using the primers
678 BR-TF390-P-F and BR-TF390-P-R. These three PCR fragments were mixed,
679 and a second round of PCR without primers was carried out. Then, a third round
680 of PCR with BR-TF390-L-F_Nest and BR-TF390-R-R_Nest was performed. The
681 resultant PCR fragments were introduced into the recipient strain RkuN16ptr1
682 (Δ*ku70::ptrA*, *pyrG*$^{-}$) according to (Jin *et al.*, 2011).

683 In *A. nidulans*, the *kojR* gene was deleted using a gene replacement
684 cassette which was constructed by *"in vivo"* recombination in *S. cerevisiae* as
685 previously described by Colot *et al.* (2006). Thus, approximately 2.0 kb from the
686 5'-UTR and 3'-UTR flanking region of the targeted ORF regions were selected for
687 primer design. The primers AN4118 (kojR)_pRS426_5UTR_fw and
688 AN4118_pRS426_3UTR_rv contained a short homologous sequence to the MCS
689 of the plasmid pRS426. Both the 5- and 3-UTR fragments were PCR-amplified
690 from *A. nidulans* genomic DNA (TNO2A3 strain). The *pyrG* gene placed within
691 the cassette as a prototrophic marker was amplified from pCDA21 plasmid using
692 the primers AN4118_5UTR_pyrG_rv and AN4118_3UTR_pyrG_fw. The cassette

693 was PCR-amplified from these plasmids utilizing TaKaRa Ex Taq™ DNA
694 Polymerase (Clontech Takara Bio) and used for *A. nidulans* transformation.

695 Complementation of the kojR gene in *A. fumigatus* was achieved via
696 cotransformation. A fragment containing the kojR gene flanked by 1-kb 5′ and 3′
697 UTR regions was PCR amplified (primers AfukojR complemented 5UTR pRS fw
698 and AfukojR complemented 3UTR pRS rv). This DNA fragment was transformed
699 into the Δ*kojR* strain along with the plasmid pPTR1 (TaKaRa Bio) containing the
700 pyrithiamine resistance ptrA gene. Mutants were selected on MM supplemented
701 with 1 µg ml−1 pyrithiamine and confirmed with PCR using the external primers
702 (AfukojR 5UTR ext fw and AfukojR 3UTR ext rv). Primer sequences are listed in
703 Supplementary Table S7.

704

705 **Screening of *A. fumigatus* transcription factor deletion strains.** A library of
706 484 *A. fumigatus* TFKO (transcription factor knock out) strains (Furukawa et al.,
707 2020) was screened for sensitivity to gliotoxin. To verify this sensitivity, gliotoxin
708 concentrations lower than the minimum inhibitory concentration (MIC) for the *A.*
709 *fumigatus* wild type strain, CEA17, (70µg / mL; Ries et al., 2020) were used.
710 Conidia were inoculated in 96-well plates at the final concentration of 10^4 spores
711 / well, in 200 µl MM supplemented or not with concentrations of gliotoxin ranging
712 from 35 µg/ml (0.5 x MIC of wt) to 70 µg/ml, and incubated at 37 °C for 48 h.
713 Three independent experiments were carried out. Validation of this screening
714 was carried out by growing sensitive strains at the concentration of 10^4 spores in
715 solid MM plates with 30 µg/ml gliotoxin at 37 °C, for 48 h.
716

717 **Gliotoxin and Bis(methylthio)gliotoxin Presence Analysis by ultra-high-**
718 **performance liquid chromatography (UHPLC) coupled to high-resolution**
719 **electrospray ionization mass spectrometry (HRESIMS).** All strains were
720 grown on Czapek Dox Agar (CDA) at 37°C in an incubator (VWR International)
721 in the dark over four days. To evaluate the biosynthesis of gliotoxin (GT) and
722 bis(methylthio)gliotoxin (bmGT) in these fungal strains, cultures were extracted
723 with organic solvents and analyzed by mass spectrometry (see below). The agar
724 plates were sprayed with MeOH, chopped with a spatula, and then the contents
725 were transferred into a scintillation vial. Afterwards, acetone (~15 ml) was added

726 to the scintillation vial, and the resulting slurry was vortexed vigorously for
727 approximately 3 min and then let too set at RT for 4 h. Next, the mixture was
728 filtered, and the resulting extract was dried under a stream of nitrogen gas.
729 HRESIMS experiments utilized a Thermo QExactive Plus mass
730 spectrometer (Thermo Fisher Scientific), equipped with an electrospray ionization
731 source. This was coupled to an Acquity UHPLC system (Waters Corp.), using a
732 flow rate of 0.3 ml/min and a BEH C_{18} column (2.1 mm x 50 mm, 1.7 µm) that
733 was operated at 40°C. The mobile phase consisted of CH_3CN–H_2O (Fischer
734 Optima LC-MS grade; both acidified with 0.1% formic acid). The gradient started
735 at 15% CH_3CN and increased linearly to 100% CH_3CN over 8 min, where it was
736 held for 1.5 min before returning to starting conditions to re-equilibrate.
737 Extracts were analyzed in biological triplicates and each of these in
738 technical triplicate using selected ion monitoring (SIM) in the positive ion mode
739 with a resolving power of 35,000. For GT, the SIM had an inclusion list containing
740 the mass $[M+H]^+$ = 327.04677, with an isolation window of 1.8 Da and a retention
741 window of 2.5 – 5.0 min. For bmGT, the SIM had an inclusion list containing the
742 mass $[M+H]^+$ = 357.09373, with an isolation window of 1.8 Da and a retention
743 window of 2.5 – 4.5 min. The extracts, gliotoxin standard (Cayman Chemical),
744 and bis(methylthio)gliotoxin standard (isolated previously; STEENWYK et al,
745 2020) were each prepared at a concentration of 2.5 mg/ml for the extracts and
746 0.01 mg/ml for the standards; all extracts were dissolved in MeOH and injected
747 with a volume of 3 µl. To eliminate the possibility for sample carryover, two blanks
748 (MeOH) were injected between every sample, and the standards were analyzed
749 at the end of of the run.
750 To ascertain the relative abundance of GT and bmGT in these samples,
751 batch process methods were run using Thermo Xcalibur (Thermo Fisher
752 Scientific). For GT, we used a mass range of 327.0437 – 327.0492 Da at a
753 retention time of 3.24 min with a 5.00 second window. For bmGT, we used a
754 mass range of 357.0928 – 357.9937 Da at a retention time of 3.30 min with a
755 5.00 second window.
756
757 **RNA extraction, RNA-sequencing, cDNA synthesis and RTqPCR.** All
758 experiments were carried out in biological triplicates and conidia (10^7) were
759 inoculated in liquid MM (*A. fumigatus* and *A. nidulans*), or in Potato Dextrose

760 Broth (*A. oryzae*). Gliotoxin was added for 3 h to the culture medium to a final
761 concentration of 5 µg/ml after strains were grown for 21 h in MM. As GT was
762 dissolved in DMSO, control cultures received the same volume of DMSO for 3 h.
763 For total RNA isolation, mycelia were ground in liquid nitrogen and total RNA was
764 extracted using TRIzol (Invitrogen), treated with RQ1 RNase-free DNase I
765 (Promega), and purified using the RNAeasy kit (Qiagen) according to the
766 manufacturer's instructions. RNA was quantified using a NanoDrop and Qubit
767 fluorometer, and analyzed using an Agilent 2100 Bioanalyzer system to assess
768 the integrity of the RNA. All RNA had an RNA integrity number (RIN) between 8.0
769 and 10 (Thermo Scientific) according to the manufacturer's protocol.
770 RNA-sequencing was carried out using Illumina sequencing. The cDNA
771 libraries were constructed using the TruSeq Total RNA with Ribo Zero (Illumina,
772 San Diego, CA, USA). From 0.1-1 µg of total RNA, the ribosomal RNA was
773 depleted and the remaining RNA was purified, fragmented and prepared for
774 complementary DNA (cDNA) synthesis, according to manufacturer
775 recommendations. The libraries were validated following the Library Quantitative
776 PCR (qPCR) Quantification Guide (Illumina). Paired-end sequencing was
777 performed on the Illumina NextSeq 500 Sequencing System using NextSeq High
778 Output (2 x 150) kit, according to manufacturer recommendations. The BioProject
779 ID in the NCBI's BioProject database is PRJNA729661.
780 For RTqPCR, the RNA was reverse transcribed to cDNA using the
781 ImProm-II reverse transcription system (Promega) according to manufacturer's
782 instructions, and the synthesized cDNA was used for real-time analysis using the
783 SYBR green PCR master mix kit (Applied Biosystems) in the ABI 7500 Fast real-
784 time PCR system (Applied Biosystems, Foster City, CA, USA). Primer sequences
785 are listed in Supplementary Table S7. RNASeq data was processed to select
786 genes for normalization of the qPCR data, applying the method of Yim *et al*.
787 (2015). Briefly, genes with a coefficient of variation smaller than 10%, behaving
788 in a normally distributed manner, and with large expression values (FPKM) were
789 selected. After experimental validation, Afu2g02680 (Putative matrix AAA
790 protease) and AN1191 [Small ubiquitin-like modifier (SUMO) protein]. For *A.*
791 *oryzae* experiments, *tubA* (AO090009000281) was used as a normalizer.
792

793 **Kojic Acid (KA) production by *A. oryzae*.** KA production by the A. oryzae
794 strains was detected by the colorimetric method verifying the intensity of the red
795 color formed by chelating ferric ions (BENTLEY, 1957; TERABAYASHI et al,
796 2010). The standard medium for KA production [0.25% (w/v) yeast extract, 0.1%
797 (w/v) K_2HPO_4, 0.05% (w/v) MgSO4–7H_2O, and 10% (w/v) glucose, pH 6.0]
798 containing 1 mM ferric ion ($FeCl_3$) was used for detecting KA production by *A.*
799 *oryzae*. The color of the medium turned red, indicating the presence of KA
800 chelated with ferric ions. This color change could be observed at around 5 days
801 after cultivation.
802

803 ## Acknowledgements

804

805 We thank São Paulo Research Foundation (FAPESP) grant numbers
806 2016/12948-7 (PAC), 2018/25217-6 (JAFF), 2017/14159-2 (LNAR), and
807 2018/10962-8 (GHG) and 2016/07870-9 (GHG), and Conselho Nacional de
808 Desenvolvimento Científico e Tecnológico (CNPq) 301058/2019-9 and
809 404735/2018-5 (GHG), both from Brazil for financial support. J.L.S. and A.R. are
810 supported by the Howard Hughes Medical Institute through the James H. Gilliam
811 Fellowships for Advanced Study program. AR's laboratory received additional
812 support from a Discovery grant from Vanderbilt University, the Burroughs
813 Wellcome Fund, the National Science Foundation (DEB-1442113), and the
814 National Institutes of Health/National Institute of Allergy and Infectious Diseases
815 (R56AI146096). S.L.K. is supported by the National Institutes of Health via the
816 National Center for Complementary and Integrative Health (F31 AT010558).

817

818 ## References

819

820 Abad, A., J. Victoria Fernández-Molina, J. Bikandi, A. Ramírez, J. Margareto et
821 al., 2010 What makes Aspergillus fumigatus a successful pathogen?
822 Genes and molecules involved in invasive aspergillosis. Rev. Iberoam.
823 Micol. 27: 155–182. https:// doi.org/10.1016/j.riam.2010.10.003.

824 Amich, J., Schafferer, L., Haas, H., and Krappmann, S. (2013). Regulation of
825 sulphur assimilation is essential for virulence and affects iron homeostasis
826 of the human-pathogenic mould *Aspergillus fumigatus*. *PLoS Pathog.*
827 9:e1003573. doi: 10.1371/journal.ppat.1003573.

828 Arias M, Santiago L, Vidal-Garcı´a M, Redrado S, Lanuza P, Comas L, et al.
829 Preparations for invasion: Modulation of host lung immunity during
830 pulmonary aspergillosis by gliotoxin and other fungal secondary
831 metabolites. Front Immunol. 2018; 9: 1–12.
832 https://doi.org/10.3389/fimmu.2018.00001 PMID: 29403488.

833 Benjamini Y, Drai D, Elmer G, Kafkafi N and Golani I. 2001. Controlling the false
834 discovery rate in behavior genetics research. *Behav Brain Res,* 125, 279-
835 284.

836 Bentley, R., 1957. Preparation and analysis of kojic acid. Methods Enzymol. 3,
837 238–241.

838 Bignell, E., T. C. Cairns, K. Throckmorton, W. C. Nierman, and N. P. Keller, 2016
839 Secondary metabolite arsenal of an opportunistic pathogenic fungus.
840 Philos. Trans. R. Soc. B Biol. Sci. 371: 20160023.
841 https://doi.org/10.1098/rstb.2016.0023.

842 Blachowicz, A., N. Raffa, J. W. Bok, T. Choera, B. Knox et al., 2020 Contributions
843 of spore secondary metabolites to UV-C protection and virulence vary in
844 different Aspergillus fumigatus strains. MBio 11: e03415-19.
845 https://doi.org/10.1128/mBio.03415–19.

846 Bok JW, Chung D, Balajee SA, Marr KA, Andes D, Nielsen KF, Frisvad JC, Kirby
847 KA, Keller NP. GliZ, a transcriptional regulator of gliotoxin biosynthesis,
848 contributes to Aspergillus fumigatus virulence. Infect Immun. 2006
849 Dec;74(12):6761-8. doi: 10.1128/IAI.00780-06. Epub 2006 Oct 9. PMID:
850 17030582; PMCID: PMC1698057.

851 Bolger AM, Lohse M and Usadel B. 2014. Trimmomatic: a flexible trimmer for
852 Illumina sequence data. *Bioinformatics,* 30 (15): 2114-20.

853 Camacho, C., Coulouris, G., Avagyan, V., Ma, N., Papadopoulos, J., Bealer, K.,
854 et al. (2009). BLAST+: architecture and applications. *BMC Bioinformatics*
855 10, 421. doi:10.1186/1471-2105-10-421.

856 Colot, H.H., Park, G., Turner, G.E., Ringelberg, C., Crew, C.M. et al. 2006. A
857 highthroughput gene knockout procedure for Neurospora reveals functions
858 for multiple transcription factors. Proc Nat Acad Sci USA 103:10352-
859 10357.

860 Davis, C., Carberry, S., Schrettl, M., Singh, I., Stephens, J. C., Barry, S. M., et al.
861 (2011). The role of glutathione S-transferase GliG in gliotoxin biosynthesis
862 in *Aspergillus fumigatus*. *Chem. Biol.* 18, 542–552. doi:
863 10.1016/j.chembiol.2010. 12.022.

864 Dolan SK, O'Keeffe G, Jones GW, Doyle S. Resistance is not futile: Gliotoxin
865 biosynthesis, functionality and utility. Trends Microbiol. 2015; 23: 419–428.
866 https://doi.org/10.1016/j.tim.2015.02.005 PMID: 25766143.

867 Dolan SK, Bock T, Hering V, Owens RA, Jones GW, Blankenfeldt W, Doyle S.
868 Structural, mechanistic and functional insight into gliotoxin *bis*-
869 thiomethylation in *Aspergillus fumigatus*. Open Biol. 2017
870 Feb;7(2):160292. doi: 10.1098/rsob.160292. PMID: 28179499; PMCID:
871 PMC5356443.

872 Dolan SK, Owens RA, O'Keeffe G, Hammel S, Fitzpatrick DA, Jones GW, Doyle
873 S. Regulation of nonribosomal peptide synthesis: *bis*-thiomethylation
874 attenuates gliotoxin biosynthesis in *Aspergillus fumigatus*. Chem Biol.
875 2014 Aug 14;21(8):999-1012. doi: 10.1016/j.chembiol.2014.07.006. PMID:
876 25126990.

877 Emms, D. M., and Kelly, S. (2019). OrthoFinder: phylogenetic orthology inference
878 for comparative genomics. *Genome Biol.* 20, 238. doi:10.1186/s13059-
879 019-1832-y.

880 Furukawa T, van Rhijn N, Fraczek M, Gsaller F, Davies E, Carr P, Gago S,
881 Fortune-Grant R, Rahman S, Gilsenan JM, Houlder E, Kowalski CH, Raj
882 S, Paul S, Cook P, Parker JE, Kelly S, Cramer RA, Latgé JP, Moye-Rowley
883 S, Bignell E, Bowyer P, Bromley MJ. The negative cofactor 2 complex is a

key regulator of drug resistance in Aspergillus fumigatus. Nat Commun. 2020 Jan 22;11(1):427. doi: 10.1038/s41467-019-14191-1. PMID: 31969561; PMCID: PMC7194077.

Galagan JE, Calvo SE, Cuomo C, Ma LJ, Wortman JR, Batzoglou S, Lee SI, Baştürkmen M, Spevak CC, Clutterbuck J, Kapitonov V, Jurka J, Scazzocchio C, Farman M, Butler J, Purcell S, Harris S, Braus GH, Draht O, Busch S, D'Enfert C, Bouchier C, Goldman GH, Bell-Pedersen D, Griffiths-Jones S, Doonan JH, Yu J, Vienken K, Pain A, Freitag M, Selker EU, Archer DB, Peñalva MA, Oakley BR, Momany M, Tanaka T, Kumagai T, Asai K, Machida M, Nierman WC, Denning DW, Caddick M, Hynes M, Paoletti M, Fischer R, Miller B, Dyer P, Sachs MS, Osmani SA, Birren BW. Sequencing of Aspergillus nidulans and comparative analysis with A. fumigatus and A. oryzae. Nature. 2005 Dec 22;438(7071):1105-15. doi: 10.1038/nature04341. PMID: 16372000.

Grahl, N., K. M. Shepardson, D. Chung, and R. A. Cramer, 2012 Hypoxia and fungal pathogenesis: to air or not to air? Eukaryot. Cell 11: 560–570. https://doi.org/10.1128/EC. 00031-12.

Hoang, D. T., Chernomor, O., von Haeseler, A., Minh, B. Q., and Vinh, L. S. (2018). UFBoot2: Improving the Ultrafast Bootstrap Approximation. *Mol. Biol. Evol.* 35, 518–522. doi:10.1093/molbev/msx281.

Jain R, Valiante V, Remme N, Docimo T, Heinekamp T, Hertweck C, Gershenzon J, Haas H, Brakhage AA. The MAP kinase MpkA controls cell wall integrity, oxidative stress response, gliotoxin production and iron adaptation in Aspergillus fumigatus. Mol Microbiol. 2011 Oct;82(1):39-53. doi: 10.1111/j.1365-2958.2011.07778.x. Epub 2011 Aug 30. PMID: 21883519; PMCID: PMC3229709.

Jin FJ, Nishida M, Hara S, Koyama Y. Identification and characterization of a putative basic helix-loop-helix transcription factor involved in the early stage of conidiophore development in Aspergillus oryzae. Fungal Genet Biol. 2011 Dec;48(12):1108-15. doi: 10.1016/j.fgb.2011.10.001. Epub 2011 Oct 10. PMID: 22008745.

915 Jun SC, Choi YH, Lee MW, Yu JH, Shin KS. The Putative APSES Transcription
916 Factor RgdA Governs Growth, Development, Toxigenesis, and Virulence
917 in Aspergillus fumigatus. mSphere. 2020 Nov 11;5(6):e00998-20. doi:
918 10.1128/mSphere.00998-20. PMID: 33177217; PMCID: PMC7657592.

919 Kafer E. 1977. Meiotic and mitotic recombination in *Aspergillus* and its
920 chromosomal aberrations. *Adv Genet,* 19 33-131.

921 Kamei, K., and A. Watanabe, 2005 Aspergillus mycotoxins and their effect on the
922 host. Med. Mycol. 43: 95–99. https://
923 doi.org/10.1080/13693780500051547.

924 Katoh, K., and Standley, D. M. (2013). MAFFT Multiple Sequence Alignment
925 Software Version 7: Improvements in Performance and Usability. *Mol. Biol.*
926 *Evol.* 30, 772–780. doi:10.1093/molbev/mst010.

927 Keller, N. P., 2019 Fungal secondary metabolism: regulation, function and drug
928 discovery. Nat. Rev. Microbiol. 17: 167–180.
929 https://doi.org/10.1038/s41579-018-0121-1.

930 König S, Pace S, Pein H, Heinekamp T, Kramer J, Romp E, et al. Gliotoxin from
931 Aspergillus fumigatus Abrogates Leukotriene B4 Formation through
932 Inhibition of Leukotriene A4 Hydrolase. Cell Chem Biol. 2019; 1–11.
933 https://doi.org/10.1016/j.chembiol.2019.01.001 PMID: 30745237.

934 Knox, B. P., A. Blachowicz, J. M. Palmer, J. Romsdahl, A. Huttenlocher et al.,
935 2016 Characterization of Aspergillus fumigatus Isolates from Air and
936 Surfaces of the International Space Station. mSphere 1: e00227-16.
937 https://doi.org/10.1128/ mSphere.00227–16.

938 Knowles SL, Mead ME, Silva LP, Raja HA, Steenwyk JL, Goldman GH, Oberlies
939 NH, Rokas A. Gliotoxin, a Known Virulence Factor in the Major Human
940 Pathogen Aspergillus fumigatus, Is Also Biosynthesized by Its
941 Nonpathogenic Relative *Aspergillus fischeri*. mBio. 2020 Feb
942 11;11(1):e03361-19. doi: 10.1128/mBio.03361-19. PMID: 32047138;
943 PMCID: PMC7018655.

944 Kopylova E, Noé L and Touzet H. 2012. SortMeRNA: fast and accurate filtering
945 of ribosomal RNAs in metatranscriptomic data. *Bioinformatics,* 28, 3211-
946 3217.

947 Latgé, J.-P., and G. Chamilos, 2019 Aspergillus fumigatus and aspergillosis in
948 2019. Clin. Microbiol. Rev. 33: e00140-18.
949 https://doi.org/10.1128/CMR.00140-18.

950 Lewis RE, Wiederhold NP, Chi J, Han XY, Komanduri K V., Kontoyiannis DP, et
951 al. Detection of gliotoxin in experimental and human aspergillosis. Infect
952 Immun. 2005; 73: 635–637. https://doi.org/10.1128/IAI. 73.1.635-
953 637.2005 PMID: 15618207.

954 Liao Y, Smyth GK and Shi W. 2013. The Subread aligner: fast, accurate and
955 scalable read mapping by seed-and-vote. *Nucleic Acids Res,* 41, e108.

956 Lind AL, Wisecaver JH, Lameiras C, Wiemann P, Palmer JM, Keller NP,
957 Rodrigues F, Goldman GH, Rokas A. Drivers of genetic diversity in
958 secondary metabolic gene clusters within a fungal species. PLoS Biol.
959 2017 Nov 17;15(11):e2003583. doi: 10.1371/journal.pbio.2003583. PMID:
960 29149178; PMCID: PMC5711037.

961 Losada, L., O. Ajayi, J. C. Frisvad, J. Yu, and W. C. Nierman, 2009 Effect of
962 competition on the production and activity of secondary metabolites in
963 Aspergillus species. Med. Mycol. 47: S88–S96.
964 https://doi.org/10.1080/13693780802409542.

965 Love MI, Huber W and Anders S. 2014. Moderated estimation of fold change and
966 dispersion for RNA-seq data with DESeq2. *Genome Biol,* 15(12):550.

967 Mead, M. E., S. L. Knowles, H. A. Raja, S. R. Beattie, C. H. Kowalski et al., 2019
968 Characterizing the Pathogenic, Genomic, and Chemical Traits of
969 Aspergillus fischeri, a Close Relative of the Major Human Fungal Pathogen
970 Aspergillus fumigatus. mSphere. 4: e00018-19.
971 https://doi.org/10.1128/mSphere.00018–19.

972 Minh, B. Q., Schmidt, H. A., Chernomor, O., Schrempf, D., Woodhams, M. D.,
973 von Haeseler, A., et al. (2020). IQ-TREE 2: New Models and Efficient

974 Methods for Phylogenetic Inference in the Genomic Era. *Mol. Biol. Evol.*
975 37, 1530–1534. doi:10.1093/molbev/msaa015.

976 Mukherjee PK, Hurley JF, Taylor JT, Puckhaber L, Lehner S, Druzhinina I,
977 Schumacher R, Kenerley CM. Ferricrocin, the intracellular siderophore of
978 Trichoderma virens, is involved in growth, conidiation, gliotoxin
979 biosynthesis and induction of systemic resistance in maize. Biochem
980 Biophys Res Commun. 2018 Oct 28;505(2):606-611. doi:
981 10.1016/j.bbrc.2018.09.170. Epub 2018 Sep 29. PMID: 30278887.

982 O'Keeffe, G., Hammel, S., Owens, R.A. *et al.* RNA-seq reveals the pan-
983 transcriptomic impact of attenuating the gliotoxin self-protection
984 mechanism in *Aspergillus fumigatus*. *BMC Genomics* **15,** 894 (2014).
985 https://doi.org/10.1186/1471-2164-15-894

986 Qiao J, Kontoyiannis DP, Calderone R, Li D, Ma Y, Wan Z, Li R, Liu W. Afyap1,
987 encoding a bZip transcriptional factor of Aspergillus fumigatus, contributes
988 to oxidative stress response but is not essential to the virulence of this
989 pathogen in mice immunosuppressed by cyclophosphamide and
990 triamcinolone. Med Mycol. 2008 Dec;46(8):773-82. doi:
991 10.1080/13693780802054215. PMID: 18608886.

992 Raffa, N., and N. P. Keller, 2019 A call to arms: Mustering secondary metabolites
993 for success and survival of an opportunistic pathogen. PLOS Pathog. 15:
994 e1007606. https://doi.org/ 10.1371/journal.ppat.1007606.

995 Revell, L. J. (2012). phytools: an R package for phylogenetic comparative biology
996 (and other things). *Methods Ecol. Evol.* 3, 217–223. doi:10.1111/j.2041-
997 210X.2011.00169.x.

998 Ries LNA, Rocha MC, de Castro PA, Silva-Rocha R, Silva RN, Freitas FZ, de
999 Assis LJ, Bertolini MC, Malavazi I, Goldman GH. The *Aspergillus*
1000 *fumigatus* CrzA Transcription Factor Activates Chitin Synthase Gene
1001 Expression during the Caspofungin Paradoxical Effect. mBio. 2017 Jun
1002 13;8(3):e00705-17. doi: 10.1128/mBio.00705-17. PMID: 28611248;
1003 PMCID: PMC5472186.

1004 Ries LNA, Pardeshi L, Dong Z, Tan K, Steenwyk JL, Colabardini AC, Ferreira
1005 Filho JA, de Castro PA, Silva LP, Preite NW, Almeida F, de Assis LJ, Dos
1006 Santos RAC, Bowyer P, Bromley M, Owens RA, Doyle S, Demasi M,
1007 Hernández DCR, Netto LES, Pupo MT, Rokas A, Loures FV, Wong KH,
1008 Goldman GH. The Aspergillus fumigatus transcription factor RglT is
1009 important for gliotoxin biosynthesis and self-protection, and virulence.
1010 PLoS Pathog. 2020 Jul 15;16(7):e1008645. doi:
1011 10.1371/journal.ppat.1008645. PMID: 32667960; PMCID: PMC7384679.

1012 Rokas A, Wisecaver JH, Lind AL. The birth, evolution and death of metabolic
1013 gene clusters in fungi. Nat Rev Microbiol. 2018 Dec;16(12):731-744. doi:
1014 10.1038/s41579-018-0075-3. PMID: 30194403.

1015 Scharf DH, Heinekamp T, Remme N, Hortschansky P, Brakhage AA, Hertweck
1016 C. Biosynthesis and function of gliotoxin in Aspergillus fumigatus. Appl
1017 Microbiol Biotechnol. 2012 Jan;93(2):467-72. doi: 10.1007/s00253-011-
1018 3689-1. Epub 2011 Nov 18. PMID: 22094977.

1019 Scharf DH, Brakhage AA, Mukherjee PK. Gliotoxin--bane or boon? Environ
1020 Microbiol. 2016 Apr;18(4):1096-109. doi: 10.1111/1462-2920.13080. Epub
1021 2015 Dec 21. PMID: 26443473.

1022 Scharf DH, Habel A, Heinekamp T, Brakhage AA, Hertweck C. Opposed effects
1023 of enzymatic gliotoxin N- and S-methylations. J Am Chem Soc. 2014 Aug
1024 20;136(33):11674-9. doi: 10.1021/ja5033106. Epub 2014 Aug 7. PMID:
1025 25062268.

1026 Schlam D, Canton J, Carreño M, Kopinski H, Freeman SA, Grinstein S. Gliotoxin
1027 Suppresses Macrophage Immune Function by Subverting
1028 Phosphatidylinositol 3,4,5-Trisphosphate Homeostasis. MBio. 2016; 7: 1–
1029 15. https://doi.org/10.1128/mBio.02242-15.

1030 Schrettl M, Kim HS, Eisendle M, Kragl C, Nierman WC, Heinekamp T, Werner
1031 ER, Jacobsen I, Illmer P, Yi H, Brakhage AA, Haas H. SreA-mediated iron
1032 regulation in Aspergillus fumigatus. Mol Microbiol. 2008 Oct;70(1):27-43.
1033 doi: 10.1111/j.1365-2958.2008.06376.x. Epub 2008 Aug 21. PMID:
1034 18721228; PMCID: PMC2610380.

1035 Schrettl M, Carberry S, Kavanagh K, Haas H, Jones GW, O'Brien J, et al. Self-
1036 protection against gliotoxin-a component of the gliotoxin biosynthetic
1037 cluster, gliT, completely protects Aspergillus fumigatus against exogenous
1038 gliotoxin. PLoS Pathog. 2010; 6.
1039 https://doi.org/10.1371/journal.ppat.1000952 PMID: 20548963.

1040 Seo H, Kang S, Park YS, Yun CW. The Role of Zinc in Gliotoxin Biosynthesis of
1041 *Aspergillus fumigatus*. Int J Mol Sci. 2019 Dec 8;20(24):6192. doi:
1042 10.3390/ijms20246192. PMID: 31817957; PMCID: PMC6940964.

1043 Sheridan, K. J., Lechner, B. E., Keeffe, G. O., Keller, M. A., Werner, E. R.,
1044 Lindner, H., et al. (2016). Ergothioneine biosynthesis and functionality in
1045 the opportunistic fungal pathogen, *Aspergillus fumigatus*. *Sci. Rep.*
1046 6:35306. doi: 10.1038/srep35306.

1047 Shwab, E. K., J. W. Bok, M. Tribus, J. Galehr, S. Graessle et al., 2007 Histone
1048 deacetylase activity regulates chemical diversity in Aspergillus. Eukaryot.
1049 Cell 6: 1656–1664. https://doi.org/ 10.1128/EC.00186-07.

1050 Steenwyk JL, Mead ME, de Castro PA, Valero C, Damasio A, Dos Santos RAC,
1051 Labella AL, Li Y, Knowles SL, Raja HA, Oberlies NH, Zhou X, Cornely OA,
1052 Fuchs F, Koehler P, Goldman GH, Rokas A. Genomic and Phenotypic
1053 Analysis of COVID-19-Associated Pulmonary Aspergillosis Isolates of
1054 Aspergillus fumigatus. Microbiol Spectr. 2021 Jun 9:e0001021. doi:
1055 10.1128/Spectrum.00010-21. Epub ahead of print. PMID: 34106569.

1056 Steenwyk JL, Mead ME, Knowles SL, Raja HA, Roberts CD, Bader O, Houbraken
1057 J, Goldman GH, Oberlies NH, Rokas A. Variation Among Biosynthetic
1058 Gene Clusters, Secondary Metabolite Profiles, and Cards of Virulence
1059 Across *Aspergillus* Species. Genetics. 2020 Oct;216(2):481-497. doi:
1060 10.1534/genetics.120.303549. Epub 2020 Aug 17. PMID: 32817009;
1061 PMCID: PMC7536862.

1062 Steenwyk, J. L.; Mead, M. E.; Knowles, S. L.; Raja, H. A.; Roberts, C. D.; Bader,
1063 O.; Houbraken, J.; Goldman, G. H.; Oberlies, N. H.; Rokas, A. Genetics
1064 2020, 216, 481-497.

1065 Smith EB, Dolan SK, Fitzpatrick DA, Doyle S, Jones GW. Towards
1066 understanding the gliotoxin detoxification mechanism: *in vivo*
1067 thiomethylation protects yeast from gliotoxin cytotoxicity. Microb Cell. 2016
1068 Feb 19;3(3):120-125. doi: 10.15698/mic2016.03.485. PMID: 28357342;
1069 PMCID: PMC5349022.

1070 Struck, A. W., Thompson, M. L., Wong, L. S., and Micklefield, J. (2012).
1071 S-adenosyl-methionine-dependent methyltransferases: highly versatile
1072 enzymes in biocatalysis, biosynthesis and other biotechnological
1073 applications. *Chembiochem* 13, 2642–2655. doi:
1074 10.1002/cbic.201200556.

1075 Tamano K, Kuninaga M, Kojima N, Umemura M, Machida M, Koike H. Use of the
1076 kojA promoter, involved in kojic acid biosynthesis, for polyketide
1077 production in Aspergillus oryzae: implications for long-term production.
1078 BMC Biotechnol. 2019 Oct 26;19(1):70. doi: 10.1186/s12896-019-0567-x.
1079 PMID: 31655589; PMCID: PMC6814975.

1080 Tekaia, F., and J.-P. Latgé, 2005 Aspergillus fumigatus: saprophyte or pathogen?
1081 Curr. Opin. Microbiol. 8: 385–392.
1082 https://doi.org/10.1016/j.mib.2005.06.017.

1083 Terabayashi Y, Sano M, Yamane N, Marui J, Tamano K, Sagara J, Dohmoto M,
1084 Oda K, Ohshima E, Tachibana K, Higa Y, Ohashi S, Koike H, Machida M.
1085 Identification and characterization of genes responsible for biosynthesis of
1086 kojic acid, an industrially important compound from *Aspergillus oryzae*.
1087 Fungal Genet Biol. 2010 Dec;47(12):953-61.

1088 Traynor AM, Sheridan KJ, Jones GW, Calera JA, Doyle S. Involvement of Sulfur
1089 in the Biosynthesis of Essential Metabolites in Pathogenic Fungi of
1090 Animals, Particularly *Aspergillus* spp.: Molecular and Therapeutic
1091 Implications. Front Microbiol. 2019 Dec 13;10:2859. doi:
1092 10.3389/fmicb.2019.02859. PMID: 31921039; PMCID: PMC6923255.

1093 Tsunawaki S, Yoshida LS, Nishida S, Kobayashi T, Shimoyama T. Fungal
1094 metabolite gliotoxin inhibits assembly of the human respiratory burst

1095 NADPH oxidase. Infect Immun. 2004; 72: 3373–3382. https://
1096 doi.org/10.1128/IAI.72.6.3373-3382.2004 PMID: 15155643.

1097 van de Veerdonk FL, Gresnigt MS, Romani L, Netea MG, Latgé JP. Aspergillus
1098 fumigatus morphology and dynamic host interactions. Nat Rev Microbiol.
1099 2017 Nov;15(11):661-674. doi: 10.1038/nrmicro.2017.90. Epub 2017 Sep
1100 18. PMID: 28919635.

1101 Vicentefranqueira R, Amich J, Marín L, Sánchez CI, Leal F, Calera JA. The
1102 Transcription Factor ZafA Regulates the Homeostatic and Adaptive
1103 Response to Zinc Starvation in *Aspergillus fumigatus*. Genes (Basel).
1104 2018 Jun 26;9(7):318. doi: 10.3390/genes9070318. PMID: 29949939;
1105 PMCID: PMC6070888.

1106 Wang DN, Toyotome T, Muraosa Y, Watanabe A, Wuren T, Bunsupa S, Aoyagi
1107 K, Yamazaki M, Takino M, Kamei K. GliA in Aspergillus fumigatus is
1108 required for its tolerance to gliotoxin and affects the amount of extracellular
1109 and intracellular gliotoxin. Med Mycol. 2014 Jul;52(5):506-18. doi:
1110 10.1093/mmy/myu007. Epub 2014 May 20. PMID: 24847038.

1111 Welch TR, Williams RM. Epidithiodioxopiperazines. occurrence, synthesis and
1112 biogenesis. Nat Prod Rep. 2014 Oct;31(10):1376-404. doi:
1113 10.1039/c3np70097f. PMID: 24816491; PMCID: PMC4162872.

1114 Wiemann, P., B. E. Lechner, J. A. Baccile, T. A. Velk, W.-B. Yin et al., 2014
1115 Perturbations in small molecule synthesis uncovers an iron-responsive
1116 secondary metabolite network in Aspergillus fumigatus. Front. Microbiol.
1117 5: 530. https://doi.org/10.3389/ fmicb.2014.00530.

1118 Winkelströter LK, Dolan SK, Fernanda Dos Reis T, Bom VL, Alves de Castro P,
1119 Hagiwara D, Alowni R, Jones GW, Doyle S, Brown NA, Goldman GH.
1120 Systematic Global Analysis of Genes Encoding Protein Phosphatases in
1121 Aspergillus fumigatus. G3 (Bethesda). 2015 May 5;5(7):1525-39. doi:
1122 10.1534/g3.115.016766. PMID: 25943523. PMCID: PMC4502386.

1123 Yim A.K., et al. Using RNA-Seq Data to Evaluate reference genes suitable for
1124 gene expression studies in soybean. PLoS One 10, e0136343 (2015).

1125 Yin, W.-B., J. A. Baccile, J. W. Bok, Y. Chen, N. P. Keller et al., 2013 A
1126 nonribosomal peptide synthetase-derived iron(III) complex from the
1127 pathogenic fungus Aspergillus fumigatus. J. Am. Chem. Soc. 135: 2064–
1128 2067. https://doi.org/10.1021/ ja311145n.

1129 Yoshizawa, K. (1999). Sake: Production and flavor. Food Rev. Int. 15,
1130 83–107.

1131

1132 ## Figure legends

1133

1134 **Figure 1 – Functional characterisation (FunCat) of significantly differently**
1135 **expressed genes (DEGs) identified by RNA-sequencing in the *A. fumigatus***
1136 **Δ*rglT* strain.** (A) FunCat analysis of DEGs up-regulated in the *A. fumigatus* wild-
1137 type and in (B) Δ*rglT* strain in comparison to the wild-type (WT) strains when
1138 exposed to 5 µg/ml GT for 3 h. (C) Heat map depicting the log2 fold change
1139 (Log2FC) of differentially expressed genes (DEGs), as determined by RNA-
1140 sequencing, and encoding enzymes present in the GT BGC required for GT
1141 biosynthesis. The gene *gtmA* was also included in this heat map. (D) Heat map
1142 depicting the Log2FC of differentially expressed genes (DEGs), as determined
1143 by RNA-sequencing, and encoding enzymes required for secondary metabolite
1144 (SM) biosynthesis. In both (C) and (D) log2FC values are based on the wild-type
1145 strain exposed to GT in comparison to the wild-type control and the Δ*rglT*
1146 exposed to GT in comparison to the wild-type exposed to GT. Heat map scale
1147 and gene identities are indicated. Hierarchical clustering was performed in MeV
1148 (http://mev.tm4.org/), using Pearson correlation with complete linkage clustering.

1149

1150 **Figure 2 – Functional characterisation (FunCat) of significantly differently**
1151 **expressed genes (DEGs) identified by RNA-sequencing in the *A. nidulans***
1152 **Δ*rglT* strain.** (A) FunCat analysis of DEGs up-regulated in the *A. nidulans* wild-
1153 type in the presence of GT when compared to the control condition, and in (B)
1154 the Δ*rglT* strain in comparison to the wild-type (WT) strain when exposed to 5
1155 µg/ml GT for 3 h. (C) Heat map depicting the log2 fold change (Log2FC) of
1156 differentially expressed homologous genes (DEHGs), as determined by RNA-

1157 sequencing, that have their expression dependent on RglT. (D) Upper panel: heat
1158 map depicting the log2 fold change (Log2FC) of 9 DEHGs and *gtmA* as
1159 determined by RNA-sequencing. Lower panel: heat map depicting the log2 fold
1160 change (Log2FC) of 9 DEHGs and *gtmA* as determined by RT-qPCR. Log2FC
1161 values are based on the *A. fumigatus* (*Afu*) or *A. nidulans* (*Ani*) wild-type strains
1162 exposed to GT when compared to the *Afu* or *Ani* wild-type control and the *Afu* or
1163 *Ani* Δ*rglT* strains exposed to GT when compared to the *Afu* or *Ani* wild-type
1164 exposed to GT. Heat map scale and gene identities are indicated. Hierarchical
1165 clustering was performed in MeV (http://mev.tm4.org/), using Pearson correlation
1166 with complete linkage clustering. For the RTqPCR experiments, the values
1167 represent the average of three independent biological repetitions (each with 2
1168 technical repetitions). (D) Pearson correlation analysis between the expression
1169 of 10 genes as measured by RTqPCR and RNA-sequencing. A positive
1170 correlation was seen for all analysed datasets.
1171

1172 **Figure 3 – Identification *A. fumigatus* TFs important for gliotoxin (GT) self-**
1173 **protection.** Strains were grown from 10^7 conidia for 2 days at 37 ^oC on minimal
1174 medium (MM) supplemented with 30 µg/ml GT before colony radial diameter was
1175 measured. The results are expressed as the radial diameter of the treatment
1176 divided by the radial diameter of the growth in the control GT-free condition. The
1177 results are the means of three repetitions ± standard deviation. Statistical analysis
1178 was performed using a one-tailed, paired t-test when compared to the control
1179 condition (*, $p < 0.005$).

1180

1181 **Figure 4 – Growth phenotypes of the *A. fumigatus* GT-sensitive**
1182 **transcription factor deletion strains.** Strains were grown from 10^7 conidia for 5
1183 days at 37 ^oC on minimal medium (MM) supplemented with the indicated
1184 compounds. The results are expressed as the radial diameter of the treatment
1185 divided by the radial diameter of the growth in the control, drug-free condition.
1186 The results are the means of three repetitions ± standard deviation. Statistical
1187 analysis was performed using a one-tailed, paired t-test when compared to the
1188 control condition (*, $p < 0.005$). (A) MM+Allyl alcohol 40 mM. (B) MM+menadione
1189 0.01 mM. (C) MM+*t*-butyl hydroxyperoxide 1 mM. (D) MM+diamide 1.25 mM. (E)

1190 MM + $FeSO_4$ 200 μM. (F) MM+BPS 200 μM+Ferrozine 300 μM. (G) MM+$ZnSO_4$
1191 200 μM. (H) MM+Phenanthroline 0.025 mM.

1192

1193 **Figure 5 – Production of GT and bmGT in the *A. fumigatus* GT-sensitive TF**
1194 **deletion strains.** (A) Relative abundance of GT and (B) bisdethiobis(methylthio)-
1195 gliotoxin (bmGT) as measured by high performance liquid chromatography
1196 coupled to mass spectrometry. Results are the average of three repetitions ±
1197 standard deviation. Statistical analysis was performed using a one-tailed, paired
1198 t-test when comparing quantities to the relative abundance of the WT strain (*, p
1199 < 0.005). (C) Heat map of the results from panels (A) and (B). Heat map scale
1200 and gene identities are indicated. Hierarchical clustering was performed in MeV
1201 (http://mev.tm4.org/), using Pearson correlation with complete linkage clustering.

1202

1203 **Figure 6 – *Aspergilli* RglT and KojR homologues are important for gliotoxin**
1204 **production and self-protection.** (A) Distribution of homologs of the gliotoxin and
1205 kojic acid biosynthetic gene clusters and of the RglT and KojR homologs amongst
1206 *Aspergillus* and *Penicillium* species. Homologs of the gliotoxin biosynthetic gene
1207 cluster are present across many (but not all) *Aspergillus* and *Penicillium* species,
1208 suggesting that the cluster was present in their common ancestor. Homologs of
1209 the kojic acid biosynthetic gene cluster are present only in *Aspergillus oryzae* and
1210 close relatives, suggesting that the cluster originated much more recently.
1211 Orthologs for RglT and KojR are broadly conserved in both genera, suggesting
1212 they were present in the *Aspergillus* – *Penicillium* common ancestor. Presence
1213 or absence of biosynthetic gene cluster homologs and of gene orthologs are
1214 depicted in black or white, respectively. (B-D) Pictures and graphs of the *A.*
1215 *fumigatus* (B), *A. nidulans* (C) and *A. oryzae* (D) wild-type, Δ*rglT*, and Δ*kojR*
1216 strains when grown for 48 h from 10^7 conidia at 37 ^oC on minimal medium (MM,
1217 *A. fumigatus*, *A. nidulans*) or PDA (*A. oryzae*) and MM/PDA+30 μg of gliotoxin.
1218 Graphs correspond to the radial diameter of the colony growth that is depicted in
1219 the pictures. Standard deviations represent the average of three biological
1220 replicates with *p < 0.05 in a one-tailed, paired t-test. (E) Detection of kojic acid

1221 (KA) production in *A. oryzae* in medium containing 1 mM ferric ion ($FeCl_3$). A red
1222 colour indicates the presence of KA chelated with ferric ions.

1223

1224 **Figure 7 – GliT and GtmA are dependent on *Aspergilli* RglT and KojR.** *A.*
1225 *fumigatus*, *A. nidulans*, and *A. oryzae* strains were grown for 20 h at 37 ^{o}C before
1226 5 µg/ml of GT was added to cultures for 3 hours. RNA was extracted from all
1227 fungal strains, reverse transcribed to cDNA and RT-qPCRs were peformed. The
1228 expression of *gtmA*, *kojR* and *rglT* in the *A. nidulans* WT, Δ*rglT* and Δ*kojR* strains
1229 could not be measured due to either the absence of the gene (*gtmA*) or the
1230 absence of quantifyable mRNA. Results are the average of three biological
1231 replicates ± standard deviation. Statistical analysis was performed using a one-
1232 tailed, paired t-test when compared to the control condition (*, $p < 0.005$). (A-D)
1233 *A. fumigatus*, *A. nidulans*, and *A. oryzae* wild-type, Δ*rglT*, and Δ*kojR* strains were
1234 grown for 21 h at 37 ^{o}C and mycelia was exposed to 5 µg/ml of GT for 3 hours.
1235 RTqPCR analysis for *kojR* (A), *rglT* (B), *gliT* (C and E), and *rglT* (D and F) genes.

1236

1237 Supplemental material

1238

1239 **Supplementary Figure S1.** Comparison of RT-qPCR-based expression profiles
1240 of selected *A. fumigatus* and *A. nidulans* genes that were significantly modulated
1241 in the RNA-sequencing experiments.

1242 **Supplementary Figure S2.** Growth of the wild-type and GT-sensitive mutants in
1243 MM with different sulfur sources. The strains were grown for 72 hs at 37 ^{o}C.

1244 **Supplementary Figure S3.** Base peak chromatograms of the strain Af293, the
1245 *A. oryzae* Δ*kojR* strain, the *A. oryzae* Δ*rglT* strain, and the wild-type (WT) *A.*
1246 *oryzae* strain grown on CDA (Czapek-Dox Agar, induces gliotoxin biosynthesis)
1247 at 37°C. Results show that the *A. oryzae* WT and deletion strains do not produce
1248 (A) gliotoxin or (B) bis(methylthio)gliotoxin. The data are presented as extracted
1249 ion chromatograms (XIC) from selected ion monitoring (SIM) using the protonated
1250 mass of gliotoxin ($C_{13}H_{15}N_2O_4S_2$; $[M+H]^+ = 327.0473$) and bis(methylthio)gliotoxin

1251 ($C_{15}H_{21}N_2O_4S_2$; $[M+H]^+$ = 357.0928) with a window of ± 5.0 ppm. GT and bmGT
1252 were detected in the *A. fumigatus* positive control strain Af293.

1253 **Supplementary Table S1.** Genes significantly differentiallly expressed in the *A.*
1254 *fumigatus* wild-type strain exposed to GT in comparison to the GT-free, control
1255 condition.

1256 **Supplementary Table S2.** Genes significantly differentiallly expressed in the *A.*
1257 *fumigatus* Δ*rglT* strain in comparison to the wild-type strain when exposed to GT.

1258 **Supplementary Table S3.** Genes significantly differentiallly expressed in the *A.*
1259 *nidulans* wild-type strain exposed to GT in comparison to the GT-free, control
1260 condition. If applicable, the *A. fumigatus* homologue is also indicated.

1261 **Supplementary Table S4.** Genes significantly differentiallly expressed in the *A.*
1262 *nidulans* Δ*rglT* strain in comparison to the wild-type strain when exposed to GT.
1263 If applicable, the *A. fumigatus* homologue is also indicated. Also shown are a list
1264 of genes that are dependent or independent on RglT for their expression.

1265 **Supplementary Table S5.** GT and bmGT production in the *A. fumigatus* wild-
1266 type and transcription factor deletion strains.
1267 **Supplementary Table S6.** Strains used in this work
1268 **Supplementary Table S7.** List of primers used in this work
1269

1270

Table 1 – List of the transcription fator mutants identified as more sensitive to gliotoxin (the domains Organization are based on http://smart.embl-heidelberg.de/).

Gene ID	Structure	Family	Gliotoxin Inhibition of the null mutant (µg/ml)
RglT (AFUA_1G09190)		GAL4-like Zn(II)2Cys6	< 35
AFUA_2G17860		GAL4-like Zn(II)2Cys6	< 35
RgdA (AFUA_3G13920)		KilA-N domain	< 35
OefC (AFUA_3G09670)		GAL4-like Zn(II)2Cys6	< 35
KojR (AFUA_5G06800)		GAL4-like Zn(II)2Cys6	< 35
SreA (AFUA_5G11260)		GATA-type zinc finger	< 35
AFUA_5G12060		GAL4-like Zn(II)2Cys6	< 35
AFUA_5G14390		GAL4-like Zn(II)2Cys6	< 35
AFUA_4G13060		ZnF_C2HC domain	< 35
AFUA_6G09870		GAL4-like Zn(II)2Cys6	< 35
Yap1 (AFUA_6G09930)		Basic-leucine zipper (bZIP)	< 35
AFUA_8G07360		GAL4-like Zn(II)2Cys6	< 35
AFUA_8G07280		GAL4-like Zn(II)2Cys6	< 35
AFUA_8G05460		Basic-leucine zipper (bZIP)	< 35
AFUA_8G03970		GAL4-like Zn(II)2Cys6	< 35
AFUA_3G01100		ZnF_C2HC domain	< 35

1281 Table 2 – Akaike Information Criterium (AIC) of model fitting for phylogenetic
1282 correlation tests

	Independent	**Dependent X**	**Dependent Y**	**Interdependent**
X: *kojR*; Y: *rglT*	0.767	0.104	0.113	0.016
X: *kojR*; Y: kojic acid BGC	0.704	0.101	0.170	0.025
X: *rglT*; Y: gliotoxin BGC	0.336	0.471	0.068	0.125

1283 BGC = biosynthetic gene cluster

1284

1285

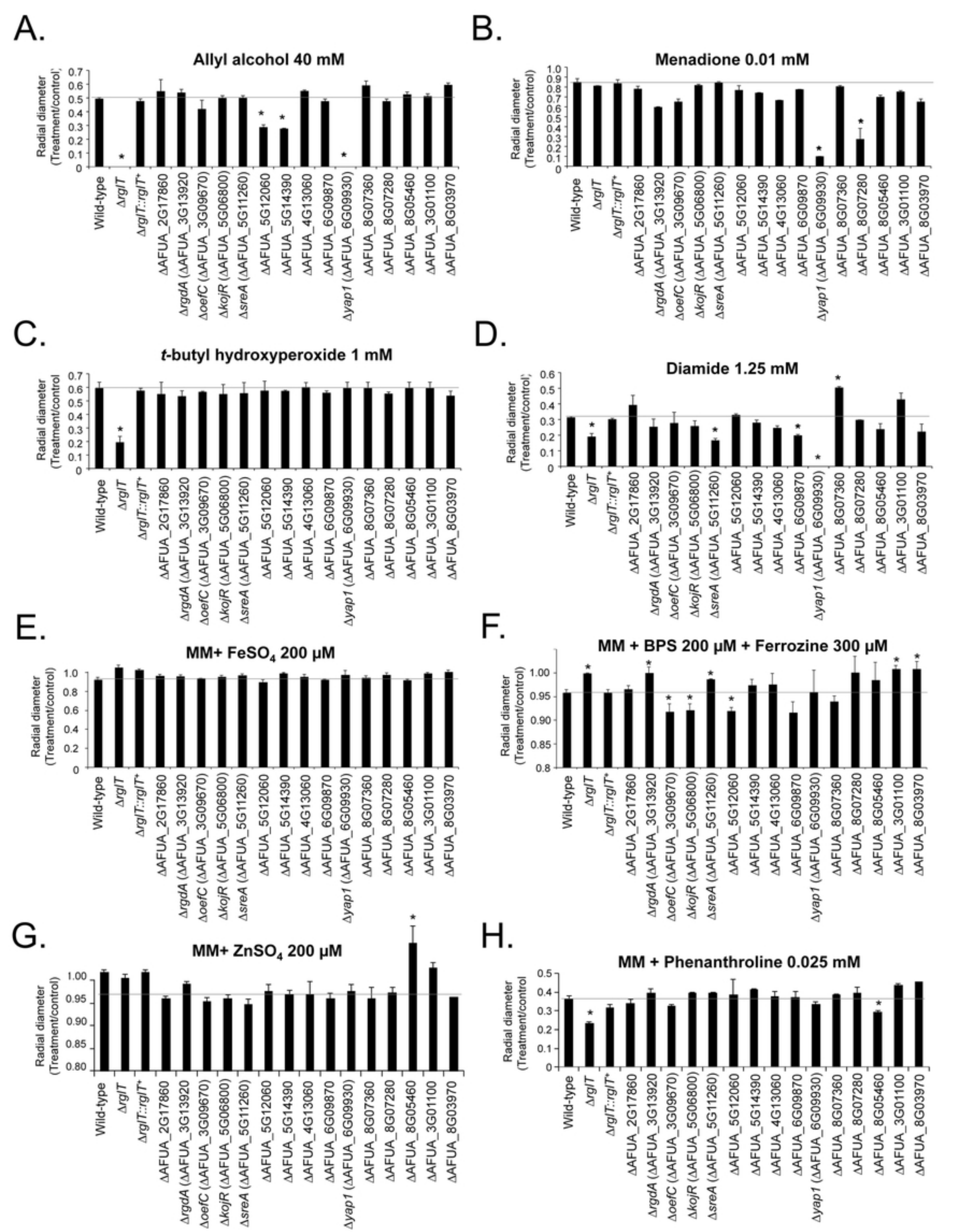
A.
Allyl alcohol 40 mM
B.
Menadione 0.01 mM
C.
t-butyl hydroxyperoxide 1 mM
D.
Diamide 1.25 mM
E.
MM+ FeSO4 200 µM
F.
MM + BPS 200 µM + Ferrozine 300 µM
G.
MM+ ZnSO4 200 µM
H.
MM + Phenanthroline 0.025 mM
Radial diameter (Treatment/control)
Wild-type
ΔrglT
ΔrglT::rglT+
ΔAFUA_2G17860
ΔrgdA (ΔAFUA_3G13920)
ΔoefC (ΔAFUA_3G09670)
ΔkojR (ΔAFUA_5G06800)
ΔsreA (ΔAFUA_5G11260)
ΔAFUA_5G12060
ΔAFUA_5G14390
ΔAFUA_4G13060
ΔAFUA_6G09870
Δyap1 (ΔAFUA_6G09930)
ΔAFUA_8G07360
ΔAFUA_8G07280
ΔAFUA_8G05460
ΔAFUA_3G01100
ΔAFUA_8G03970

Figure 4

A.

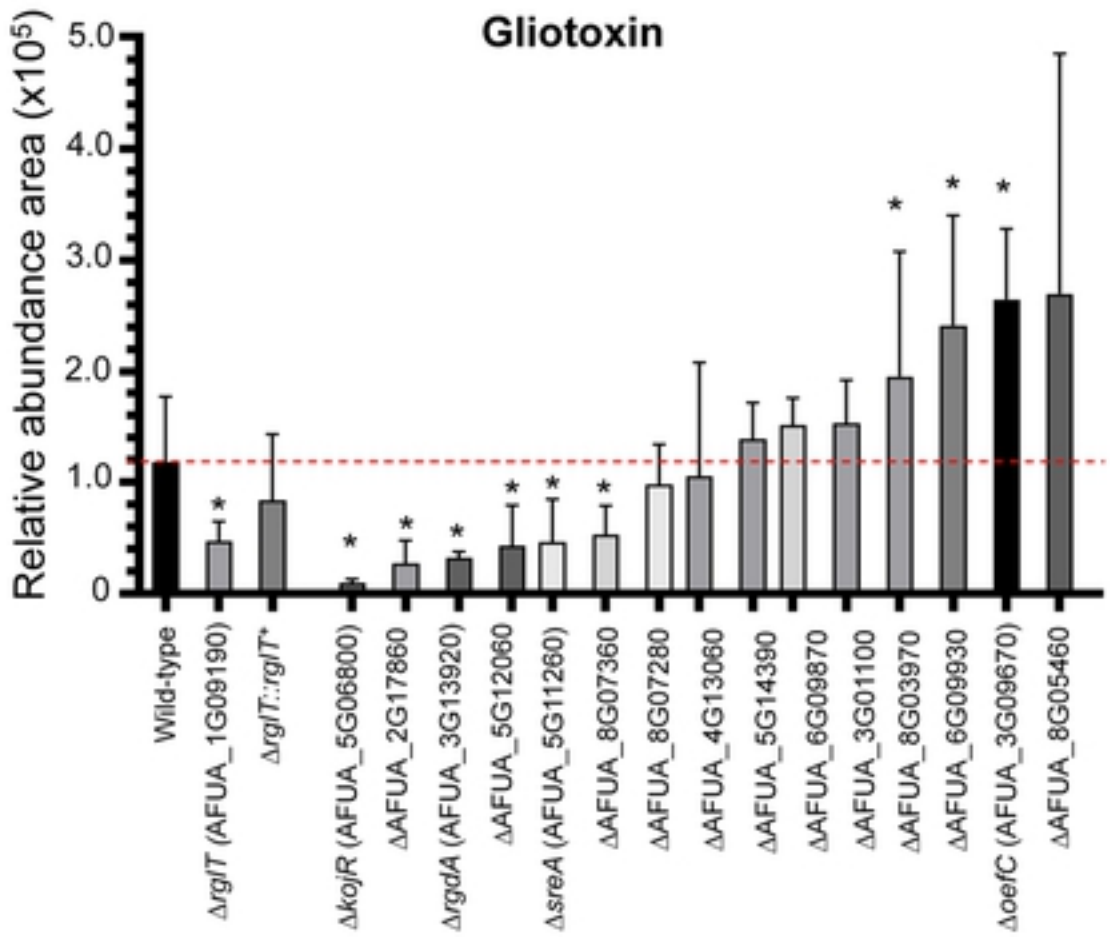
Gliotoxin
Relative abundance area (x10^5)
5.0
4.0
3.0
2.0
1.0
0
Wild-type
ΔrglT (AFUA_1G09190)
ΔrglT::rglT+
ΔkojR (AFUA_5G06800)
ΔAFUA_2G17860
ΔrgdA (AFUA_3G13920)
ΔAFUA_5G12060
ΔsreA (AFUA_5G11260)
ΔAFUA_8G07360
ΔAFUA_8G07280
ΔAFUA_4G13060
ΔAFUA_5G14390
ΔAFUA_6G09870
ΔAFUA_3G01100
ΔAFUA_8G03970
ΔAFUA_6G09930
ΔoefC (AFUA_3G09670)
ΔAFUA_8G05460

B.

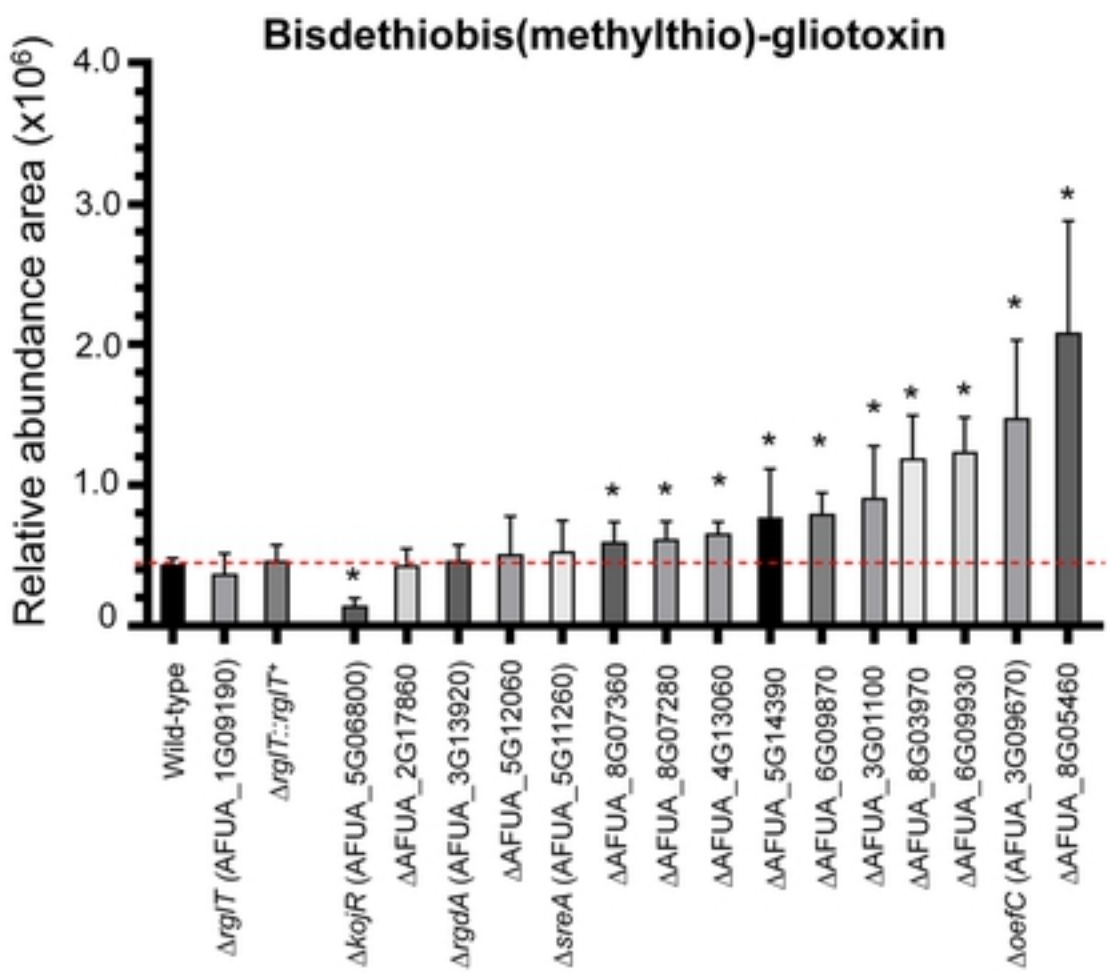
Bisdethiobis(methylthio)-gliotoxin
Relative abundance area (x10^6)
4.0
3.0
2.0
1.0
0
Wild-type
ΔrglT (AFUA_1G09190)
ΔrglT::rglT+
ΔkojR (AFUA_5G06800)
ΔAFUA_2G17860
ΔrgdA (AFUA_3G13920)
ΔAFUA_5G12060
ΔsreA (AFUA_5G11260)
ΔAFUA_8G07360
ΔAFUA_8G07280
ΔAFUA_4G13060
ΔAFUA_5G14390
ΔAFUA_6G09870
ΔAFUA_3G01100
ΔAFUA_8G03970
ΔAFUA_6G09930
ΔoefC (AFUA_3G09670)
ΔAFUA_8G05460

C.

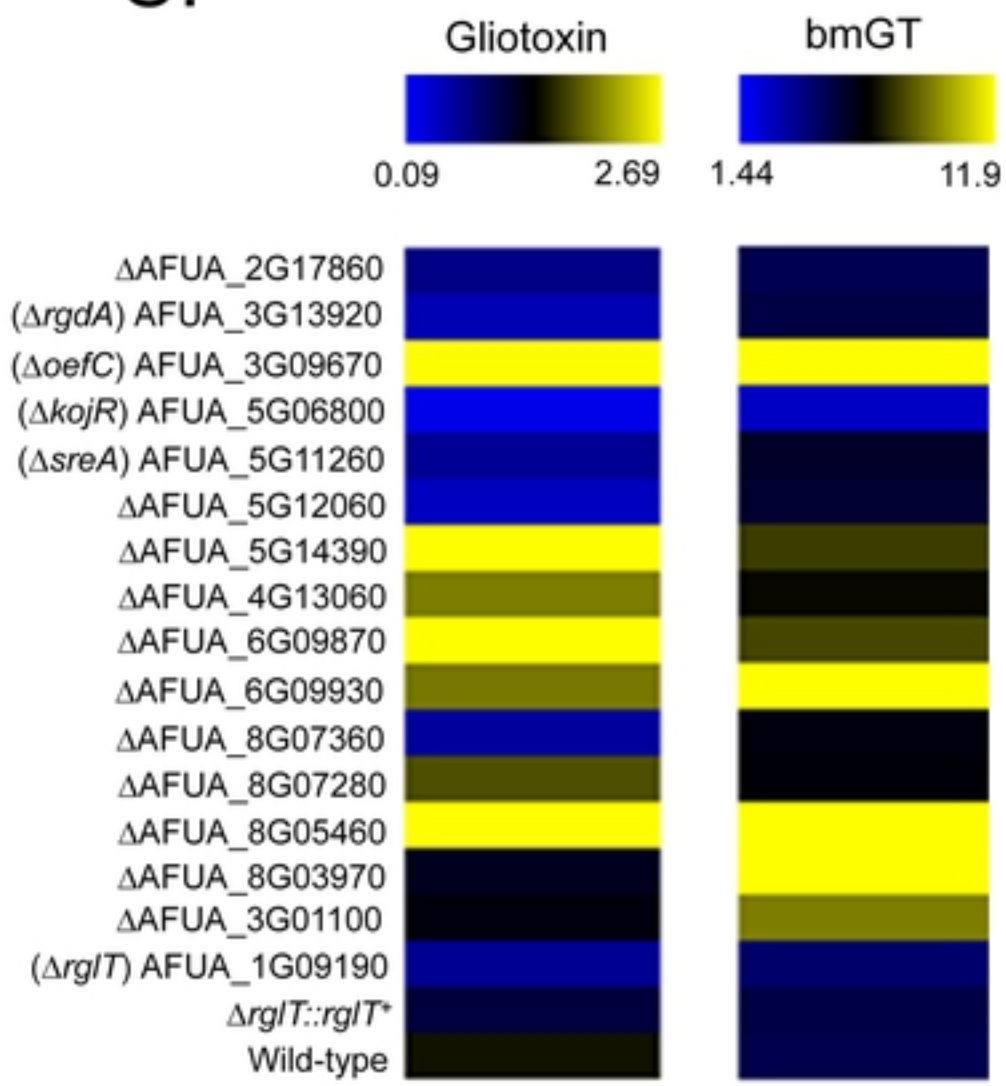
Gliotoxin
0.09
2.69
bmGT
1.44
11.9
ΔAFUA_2G17860
(ΔrgdA) AFUA_3G13920
(ΔoefC) AFUA_3G09670
(ΔkojR) AFUA_5G06800
(ΔsreA) AFUA_5G11260
ΔAFUA_5G12060
ΔAFUA_5G14390
ΔAFUA_4G13060
ΔAFUA_6G09870
ΔAFUA_6G09930
ΔAFUA_8G07360
ΔAFUA_8G07280
ΔAFUA_8G05460
ΔAFUA_8G03970
ΔAFUA_3G01100
(ΔrglT) AFUA_1G09190
ΔrglT::rglT+
Wild-type

Figure 5

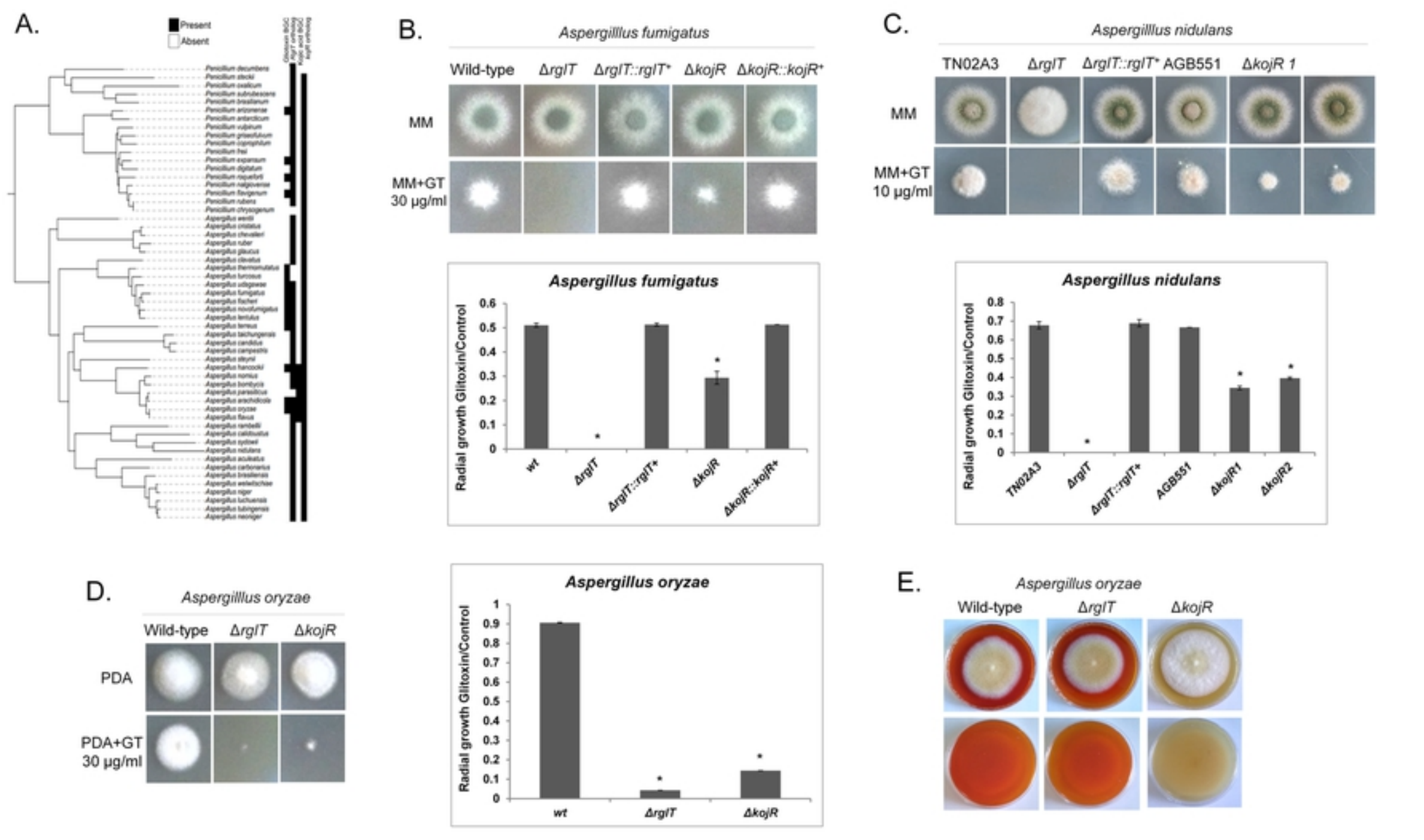
A.
Present
Absent
B.
Aspergilllus fumigatus
Wild-type
ΔrglT
ΔrglT::rglT+
ΔkojR
ΔkojR::kojR+
MM
MM+GT
30 µg/ml
Aspergillus fumigatus
Radial growth Glitoxin/Control
wt
ΔrglT
ΔrglT::rglT+
ΔkojR
ΔkojR::kojR+
C.
Aspergilllus nidulans
TN02A3
ΔrglT
ΔrglT::rglT+ AGB551
ΔkojR 1
MM
MM+GT
10 µg/ml
Aspergillus nidulans
Radial growth Glitoxin/Control
TN02A3
ΔrglT
ΔrglT::rglT+
AGB551
ΔkojR1
ΔkojR2
D.
Aspergilllus oryzae
Wild-type
ΔrglT
ΔkojR
PDA
PDA+GT
30 µg/ml
Aspergillus oryzae
Radial growth Glitoxin/Control
wt
ΔrglT
ΔkojR
E.
Aspergillus oryzae
Wild-type
ΔrglT
ΔkojR

Figure 6

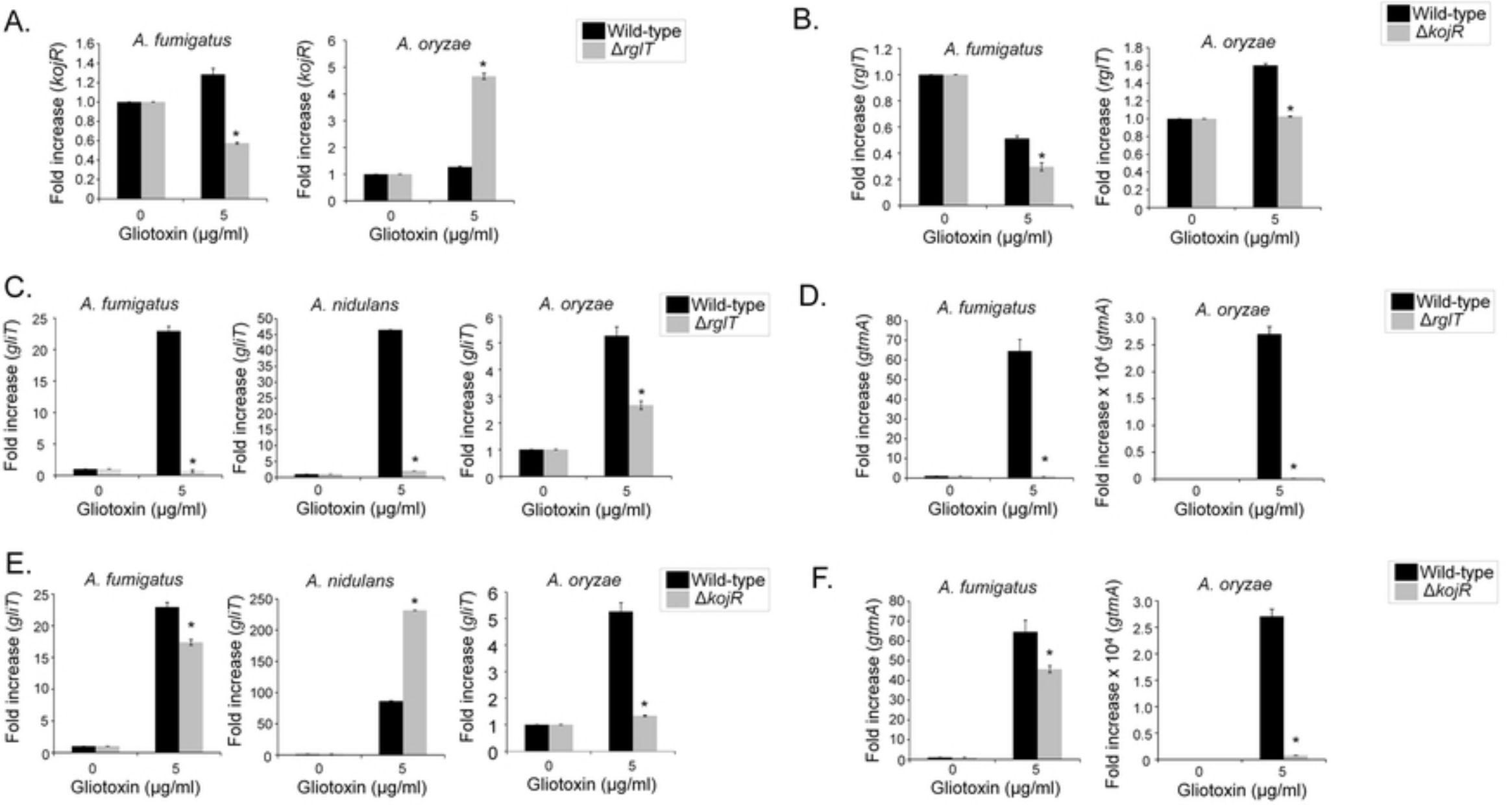
A.
A. fumigatus
A. oryzae
Wild-type
ΔrglT
Fold increase (kojR)
Gliotoxin (µg/ml)
B.
Wild-type
ΔkojR
Fold increase (rglT)
C.
A. nidulans
Fold increase (gliT)
D.
Fold increase (gtmA)
Fold increase x 10⁴ (gtmA)
E.
F.

Figure 7

A.

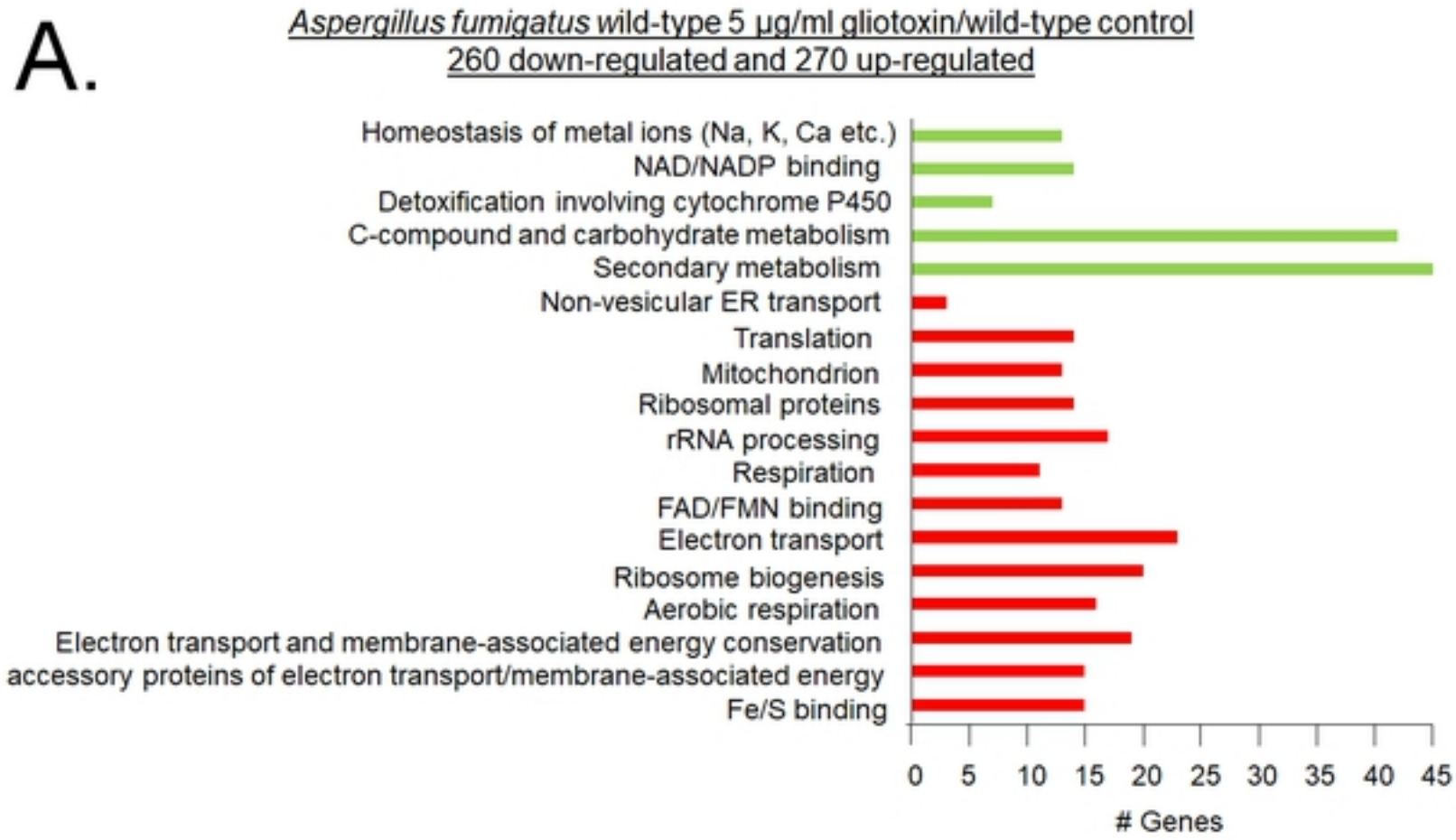

B.

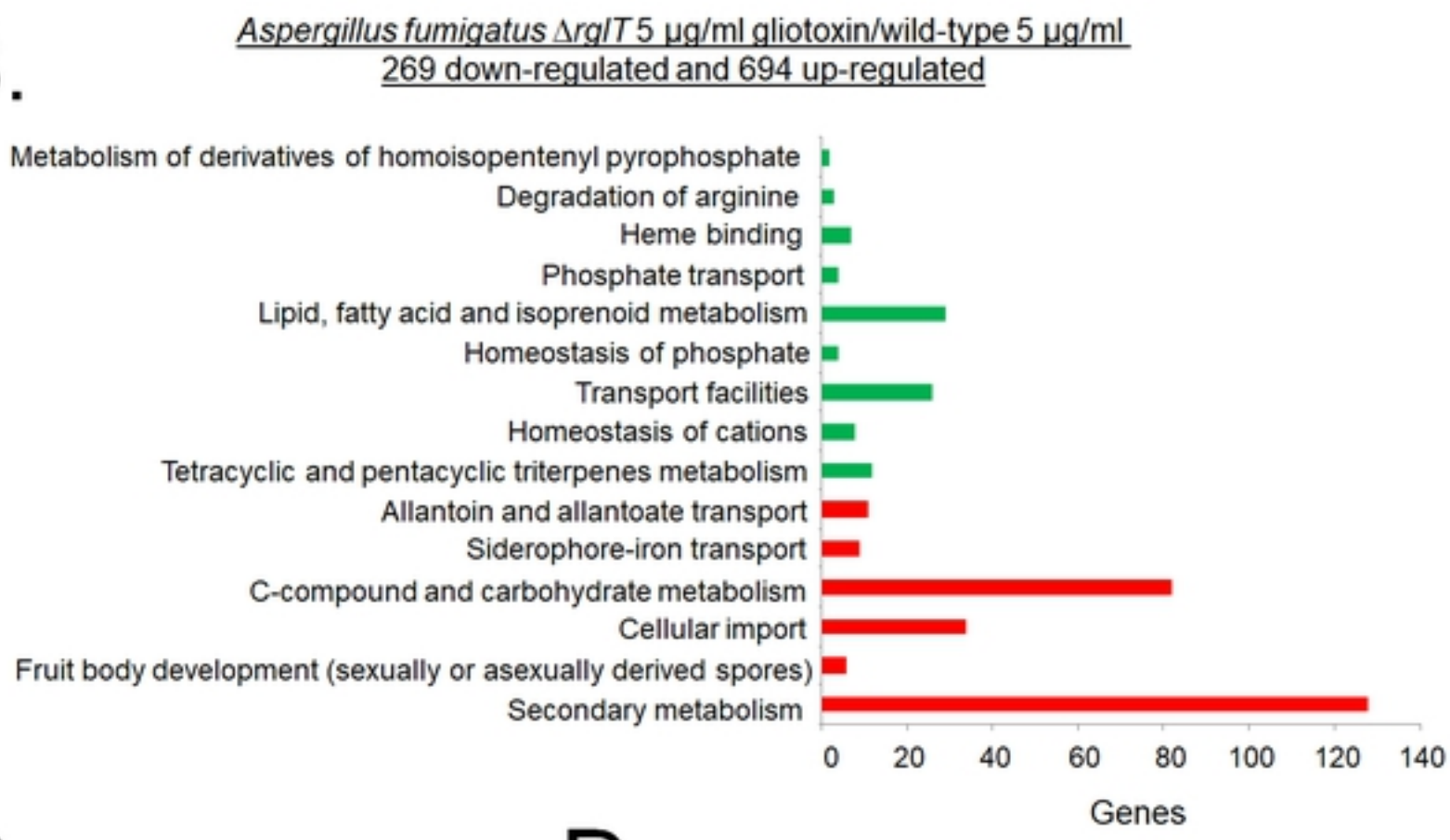

C.

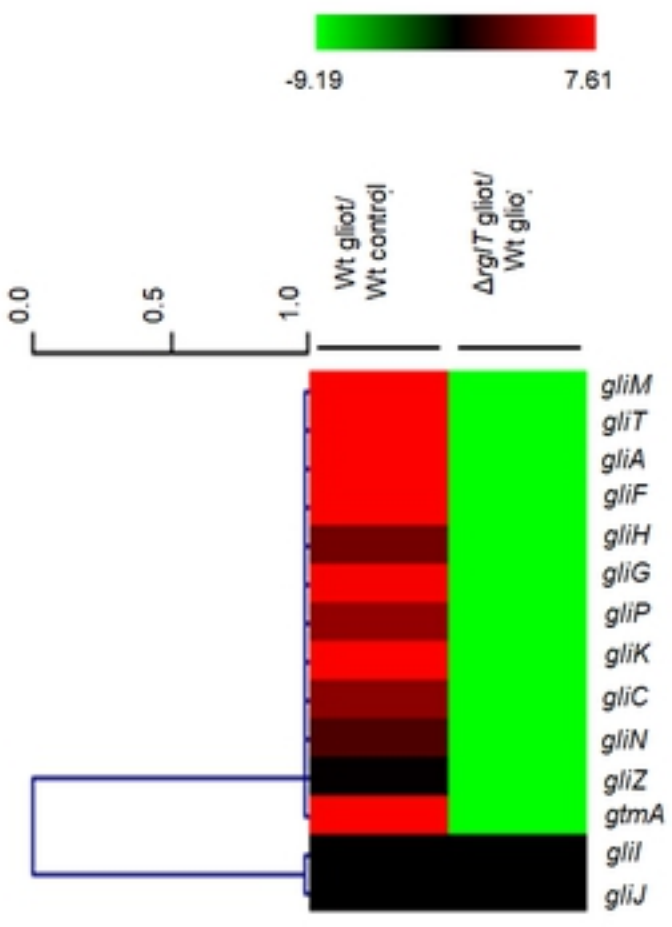

D.

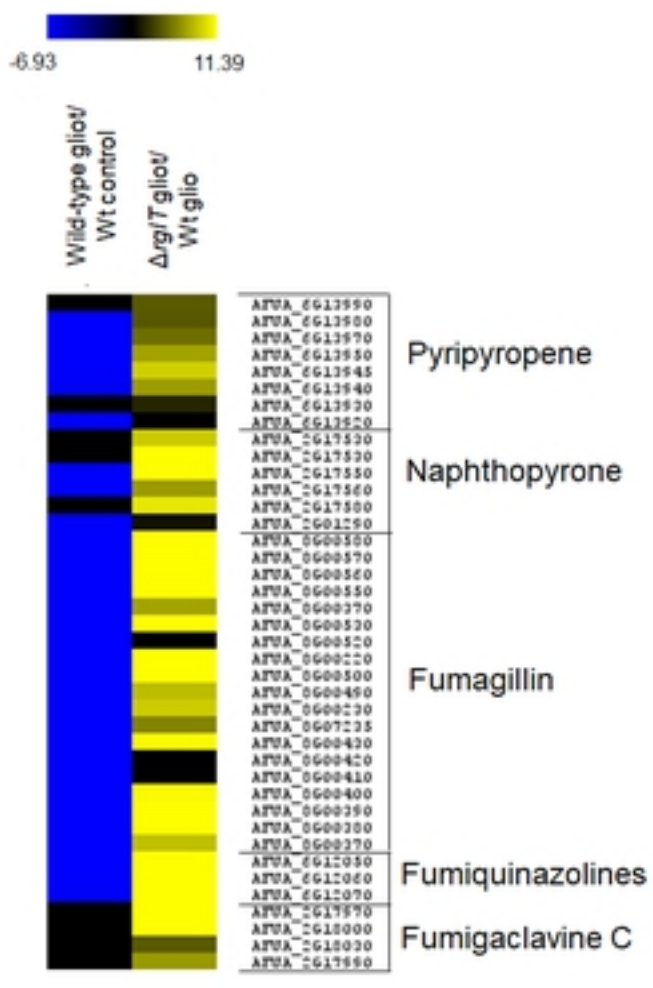

Figure 1

A.

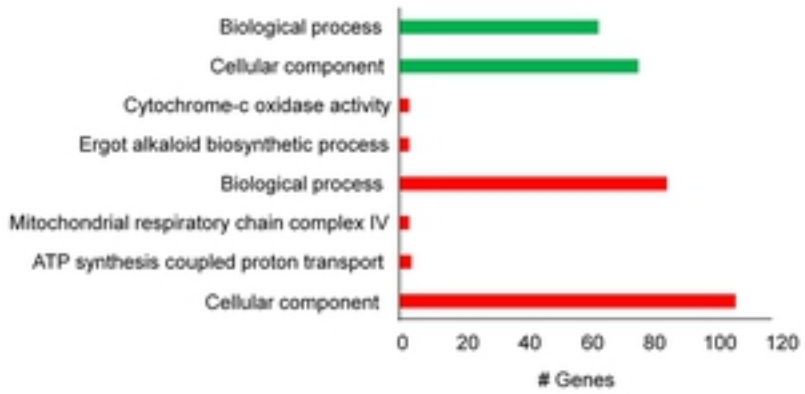

B.

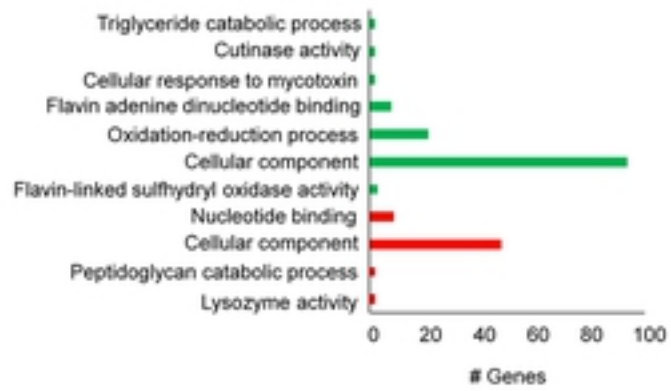

C.

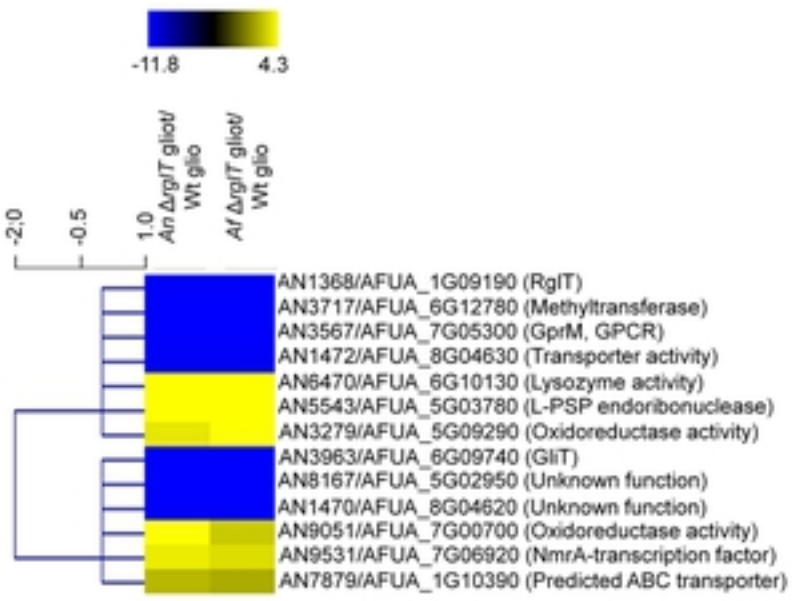

D.

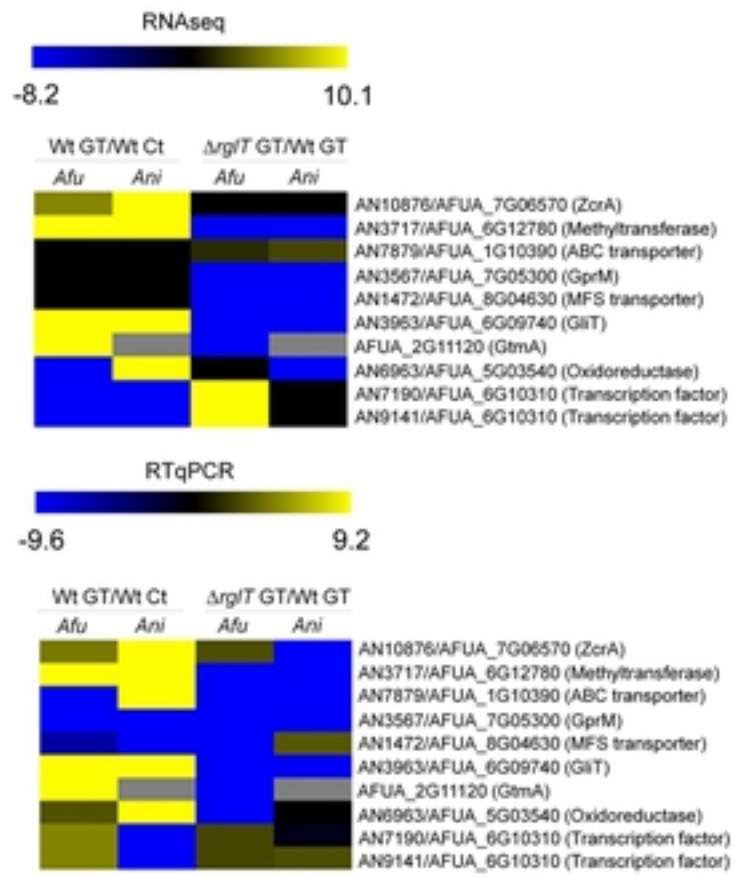

E.

RNA seq x RTqPCR				
	A. fumigatus		*A. nidulans*	
	wt glio x wt control	ΔrglT glio x wt glio	wt glio x wt control	ΔrglT glio x wt glio
Pearson r				
r	0.896	0.9188	0.952	0.9146
95% confidence interval	0.6111 to 0.9754	0.6862 to 0.9810	0.7827 to 0.9901	0.6380 to 0.9822
R squared	0.8028	0.8443	0.9063	0.8365
P value				
P (two-tailed)	0.0005	0.0002	<0.0001	0.0006
P value summary	***	***	****	***
Significant? (alpha = 0.05)	Yes	Yes	Yes	Yes
Number of XY Pairs	10	10	9	9

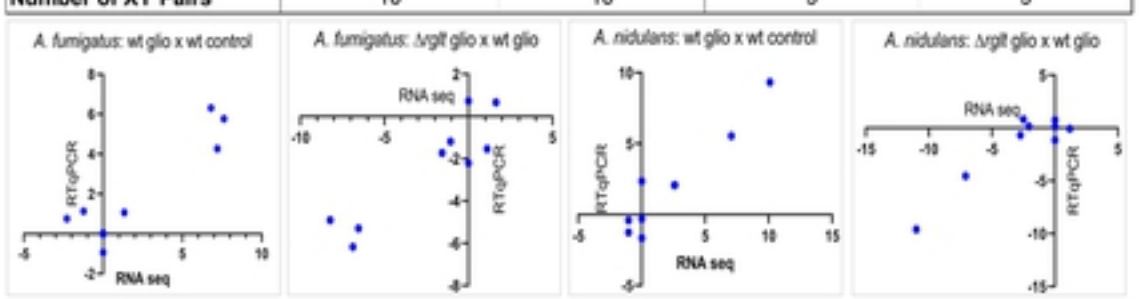

Figure 2

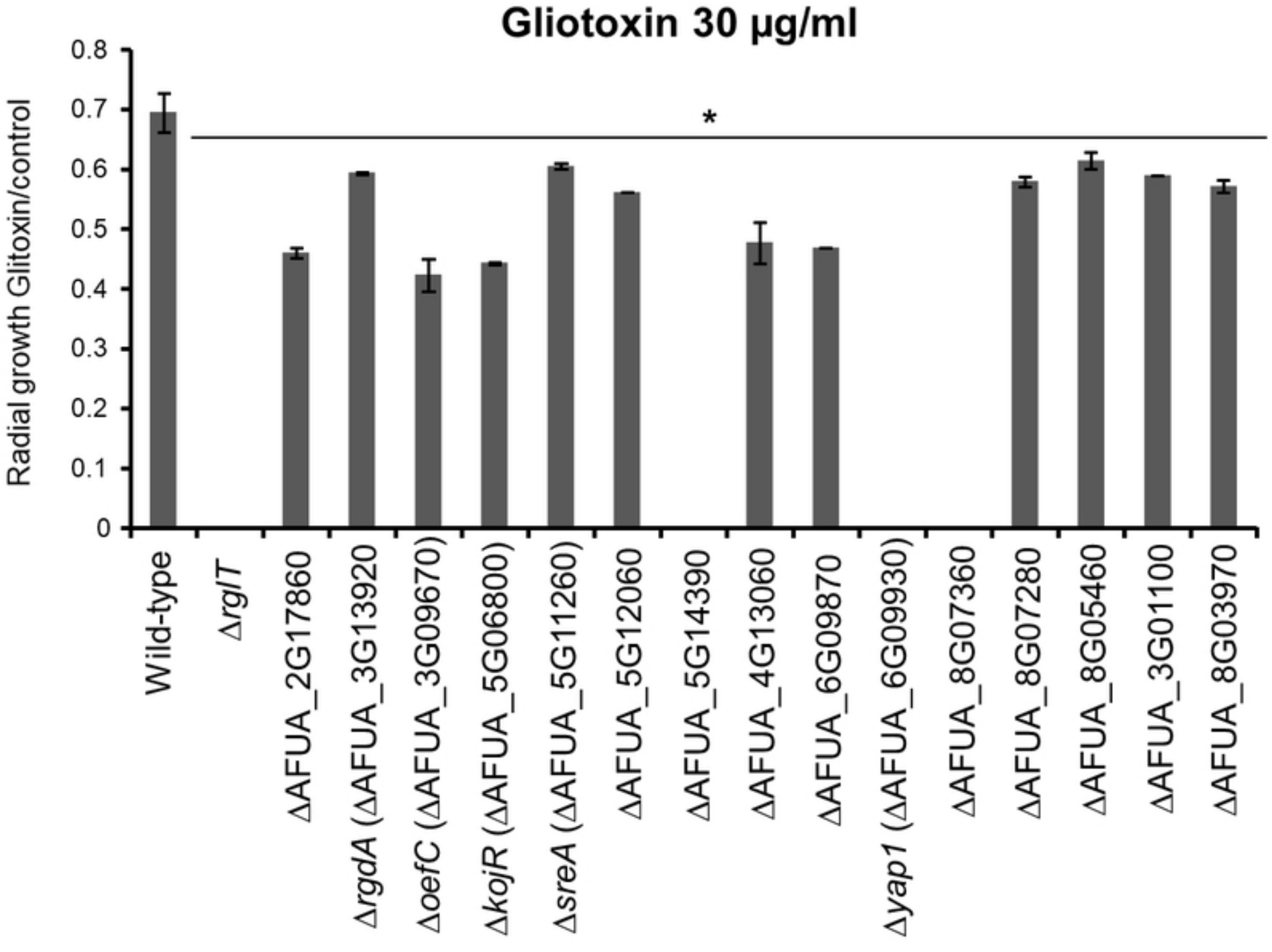
Gliotoxin 30 µg/ml
Radial growth Glitoxin/control
0.8
0.7
0.6
0.5
0.4
0.3
0.2
0.1
0
*
Wild-type
ΔrglT
ΔAFUA_2G17860
ΔrgdA (ΔAFUA_3G13920
ΔoefC (ΔAFUA_3G09670)
ΔkojR (ΔAFUA_5G06800)
ΔsreA (ΔAFUA_5G11260)
ΔAFUA_5G12060
ΔAFUA_5G14390
ΔAFUA_4G13060
ΔAFUA_6G09870
Δyap1 (ΔAFUA_6G09930)
ΔAFUA_8G07360
ΔAFUA_8G07280
ΔAFUA_8G05460
ΔAFUA_3G01100
ΔAFUA_8G03970

Figure 3